Modeling Salinity Fluxes in the Nueces Delta

by

Zhi Li and Ben R. Hodges

Submitted to:

Texas Water Development Board

Interagency Cooperation Contract

TWDB No. 1400011719

October 30, 2015

UTA 1400011719
Final Report

Executive Summary

This report documents the work accomplished in FY15 under TWDB Interagency Contract 1400011719 to improve and extend the Nueces Delta Hydrodynamic Model (NDHM). The project goals were (i) model calibration and validation, (ii) analysis of freshwater pumping, and (iii) extending the model to include Nueces Bay.

The study shows that calibration of the NDHM by adjusting the bottom roughness does not have significant global effects on the model predictions. This result is consistent with the fluxes through the delta being primarily constrained by topography, such that the model's representation of flow channels and embankment blockages is more important than the roughness (or drag coefficient). Model validation analyses (comparison to field observations) indicate the critical shortcomings in the present model are (i) lack of evaporation and porewater salinity processes, and (ii) narrow channels that have been artificially widened to maintain connectivity, but hence carry higher flows and drain the upper delta too quickly. Without evaporation and porewater salinity processes, the NDHM cannot represent the creation of high salinity concentrations within the Nueces Delta. These processes likely account for the model's bias towards lower salinity than observed (particularly in the upper delta). Problems with widening small channels (necessary for the 30×30 m grid resolution) can be solved in the future by developing an approach to relate local channel drag coefficients to the artificial channel widening.

The NDHM was used to analyze 18 different combinations of freshwater pumping, tides, and winds. The results showed that using a single pump was the most "effective," in terms of the ratio of inundation area to freshwater volume supplied. However, it is not clear that this ratio is the best metric for judging inundation performance, as the single pump cases did not flood (in the model) some of the broader areas that are of ecological importance. It is recommended that TWDB and the Coastal Bend Bays and Estuaries Program (CBBEP) develop target inundation – both in terms of desired acreage and locations within the delta – that can be used for more detailed evaluation of pumping.

The project further attempted to extend the Nueces Delta model to include all of Nueces Bay. The size of the model and computational costs made it impractical for the desktop workstations used by the research team. Future work to include Nueces Bay will require either (i) porting the model to a supercomputer, GPU computer, or multi-node parallel computer, (ii) developing a coupling system for separate bay and delta models that can be run in parallel, or (iii) adapting the model to allow coarser grid resolution in the bay than in the delta.
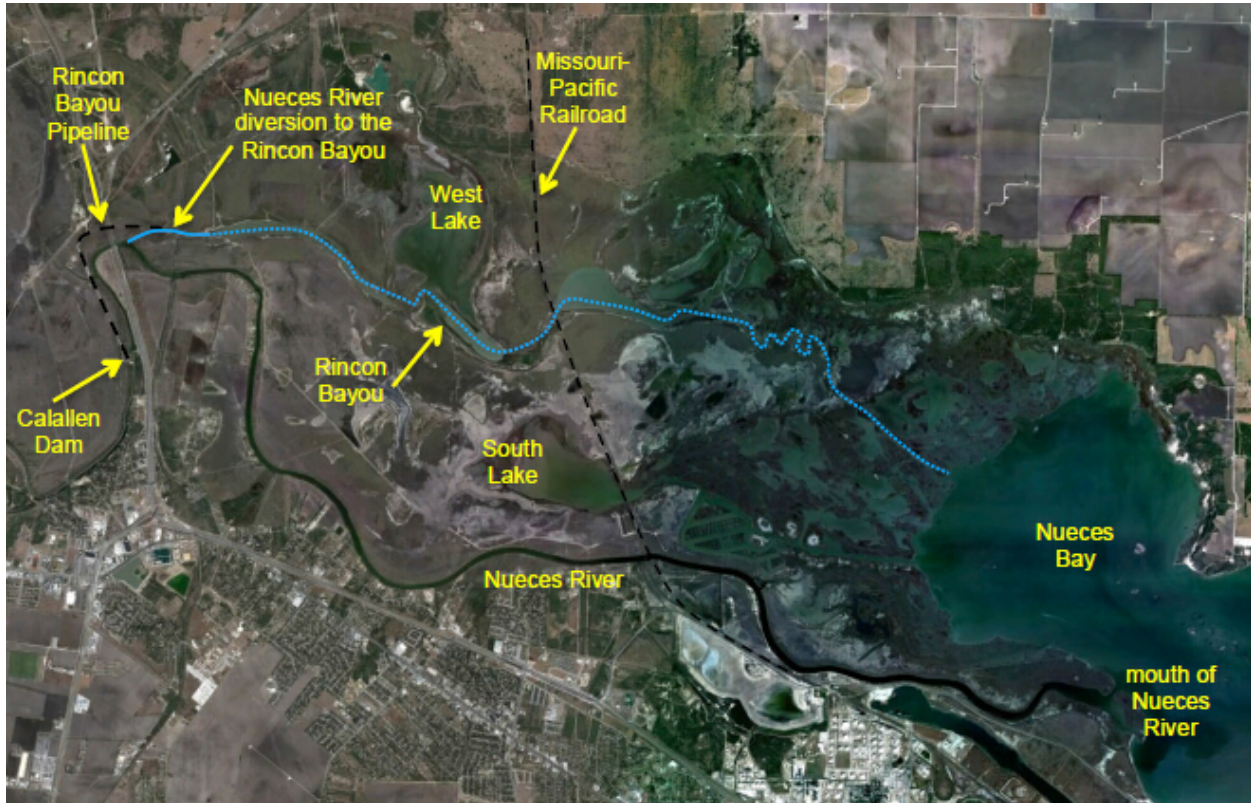
Contents

Figure 1: The Nueces Delta and the upper section of Nueces Bay from Hodges et al. [2012].

1 Introduction

This report provides the results of a study to: (i) calibrate and validate the existing Nueces Delta Hydrodynamic Model, (ii) evaluate several freshwater pumping scenarios to provide insight into the relationship between pumped flow rates, volumes, and timing, and (iii) extend the existing hydrodynamic model to all of Nueces Bay.

Nueces Bay and the Nueces River Delta (Fig. 1) have been assessed as ecologically unsound due to episodic high salinities that are detrimental to aquatic flora and fauna. [BBEST, 2011, Hodges et al., 2012]. The primary cause of increased salinity is the reduction of overbanking freshwater inflows associated with upstream dam operations in the Nueces River basin. Managing the dam operations to provide large over-banking flows that mimic natural hydrology does not appear a viable strategy due to increasing stresses on the local water supply. As a more focused approach to supplying freshwater to the delta, a pump and piping system was built in 2007 to deliver fresh water from Nueces River (upstream of the Calallen saltwater barrier) to the upstream end of the Rincon Bayou. Shortly thereafter, the Nueces Delta Hydrodynamic Model (NDHM) was created to study the hydrodynamics of freshwater and saltwater fluxes through the delta [Ryan and Hodges, 2011a].

The NDHM can be used to represent the effects of wind, tide, and freshwater inflows on the salinity distribution throughout the delta. The long-term goal for the NDHM has been to provide a better understanding

4

of the effects of pumped inflows for efficient operation. The NDHM was first tested in 2011 but was not calibrated or validated at that time as field data was insufficient. However, in a 15-month field study during 2012-13, the Texas Water Development Board (TWDB) collected salinity, water levels and flow velocities at 18 locations in Nueces Delta [Schoenbaechler et al., 2014]. This data provides the basis for the present work in calibrating and validating the NDHM.

This report provides a discussion on methods (§2) that complements the Ryan and Hodges [2011a] report on the initial development of the NDHM. Calibration (§3) and validation (§4) of the model are presented, with comparisons to the data set of [Schoenbaechler et al., 2014] for a 12-month simulation. Analyses of a range of freshwater pumping scenarios are analyzed in §5. The problems associated with extending the model to include Nueces Bay are discussed in §6. A summary section (§7) includes recommendations for future work.

2 Methods

2.1 Overview

The NDHM is a customized version of the Fine Resolution Environmental Hydrodynamics Model (Frehd), which was developed at Center for Research in Water Resources, University of Texas at Austin. Details on the NDHM can be found in Ryan and Hodges [2011a,b]. The Frehd code that underlies the NDHM is a Matlab scripting code that is an implementation of computational methods derived from works of Hodges et al. [2000], Rueda et al. [2007], Hodges and Rueda [2008] and Wadzuk and Hodges [2009]. The model represents bathymetry with a uniform rectilinear Cartesian grid, typically with relatively fine grid resolution (e.g. 15 x 15 m in Ryan and Hodges [2011a]). The numerical method is a mass-conservative hybrid finite difference/finite-volume formulation. A semi-implicit predictor/corrector scheme is used for the free-surface/momentum solution to allow stability with the local Courant-Friedrichs-Lewy (CFL) number exceeding unity. Scalar transport (e.g. salt concentration) uses a local subtime-stepping approach that provides conservative transport for CFL > 1 [Hodges, 2014]. The underlying Frehd code is capable of either 2D or 3D implementation, with solutions of either hydrostatic or the full non-hydrostatic Navier-Stokes equations. For the NDHM, the model is configured as 2D and hydrostatic.

Applying the NDHM for a particular time interval requires a model bathymetry (§2.2), initial conditions (§2.3), boundary conditions (§2.4), and bottom roughness (§3). Data for initial conditions and calibration are based on sensors from the TWDB field study, with locations as shown in Fig. 2.

2.2 Bathymetry

A 1×1 m Digital Elevation Model (DEM) derived from lidar data was previously prepared by J. Gibeaut at Texas A&M University – Corpus Christi. For the original NDHM, this bathymetry was coarsened to 15×15 m and the blocking effects of the railroad dike were manually inserted as edge features [Ryan and Hodges, 2011a]. We found it necessary to further coarsen the bathymetry to 30×30 m to provide reasonable model run times for calibration, evaluating flow scenarios, and connecting the the delta with Nueces Bay for the new Nueces Delta and Bay Hydrodynamic Model. However, at the coarser resolution, the model bathymetry prepared by simple averaging (or filtering) from the fine resolution lidar DEM will lose critical blocking (e.g., embankment) and channel features that are critical to the flow connectivity. To solve this
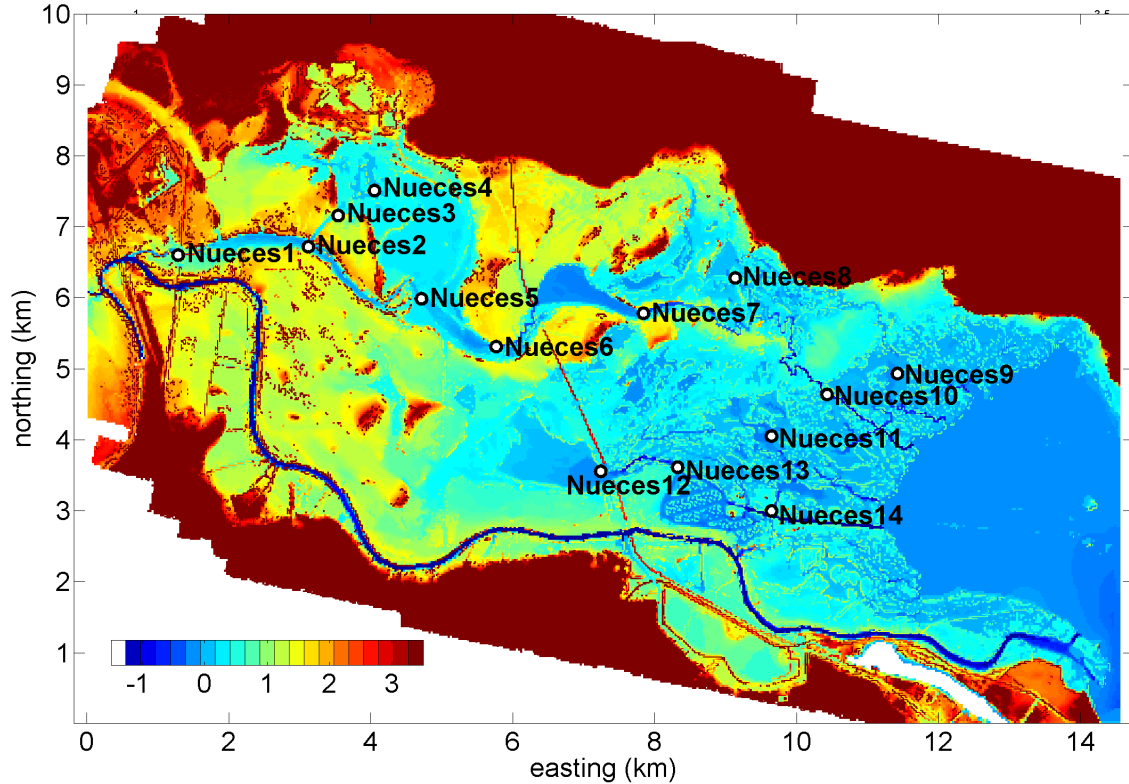
Figure 2: Location of TWDB data monitoring stations: Nueces1 through Nueces14. Topographic elevations are measured in meters above NAVD88.

problem, we created an automated method to (i) identify channels and blocking edges in the 1×1 m lidar DEM, and (ii) translate these features to a coarser grid [Hodges, 2015]. Figure 3 provides a comparison of the original lidar DEM, the 30×30 model DEM with blocking and channel features, and the 30×30 DEM using a median filter without blocking and channel algorithms over a section of the delta. It can be seen that the DEM with the blocking and channel features provides a reasonable representation of the complex topography within the delta.

The key drawback of the coarser grid resolution is that the channel widths become distorted. As shown in Fig. 4, the narrow channel connecting the middle Rincon Bayou to North Lake in the upper panel (fine resolution) is represented as a wider channel in the lower panel (coarse resolution). As wider channels allow greater flows, this effect will distort the flow rates through narrow channels. However, this result is preferable to complete blockage of the channel that occurs if the average landscape elevation is used to represent a channel narrower than the grid resolution. We are presently working on an approach to account for this distortion through automatic adjustment of the channel roughness. However, this work is preliminary and has not been used in any of the modeling results herein.
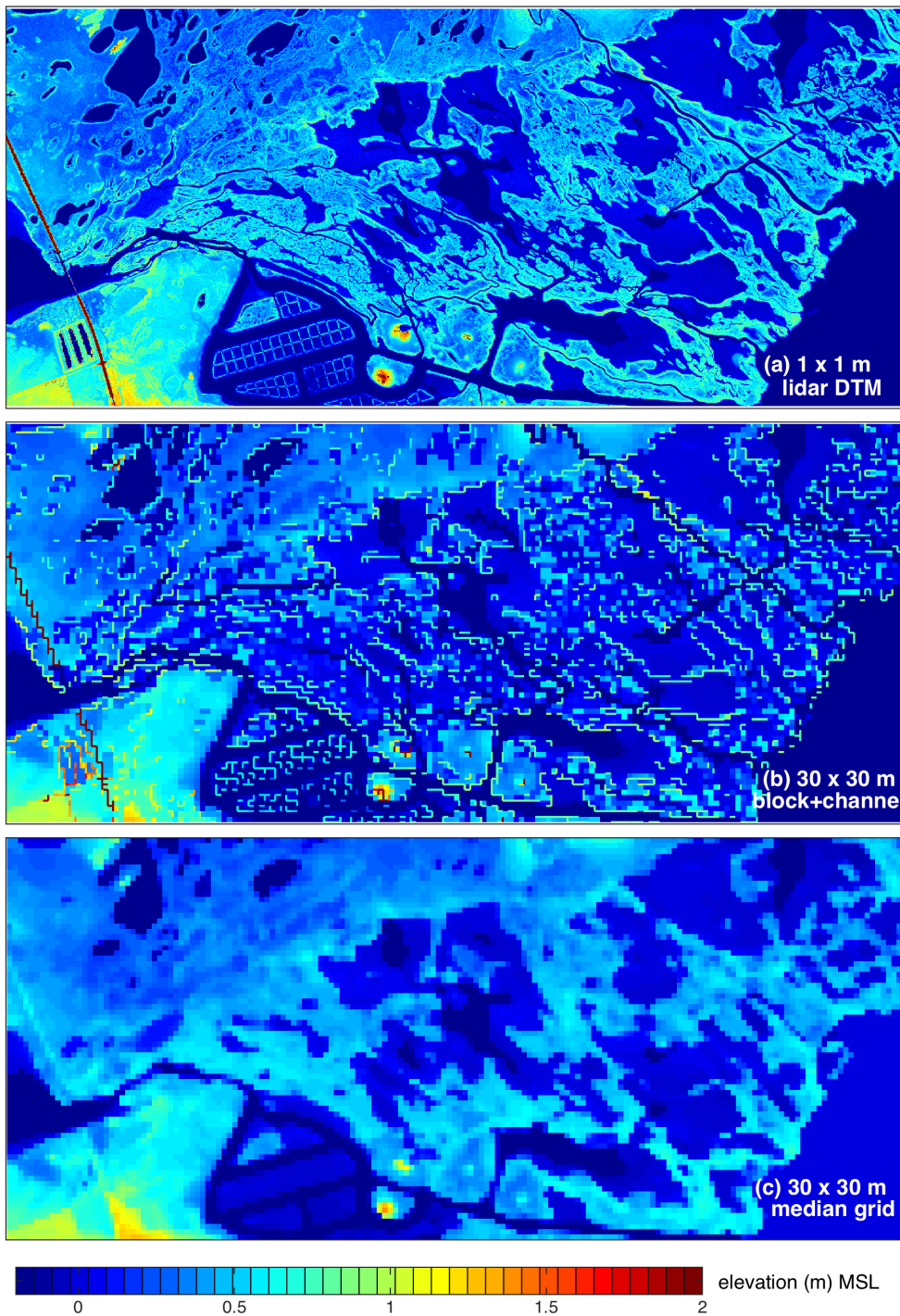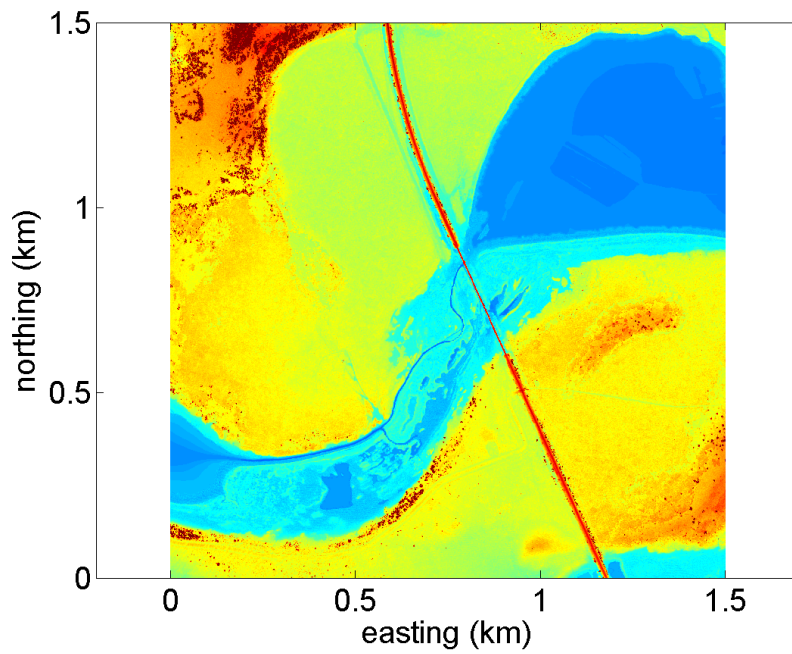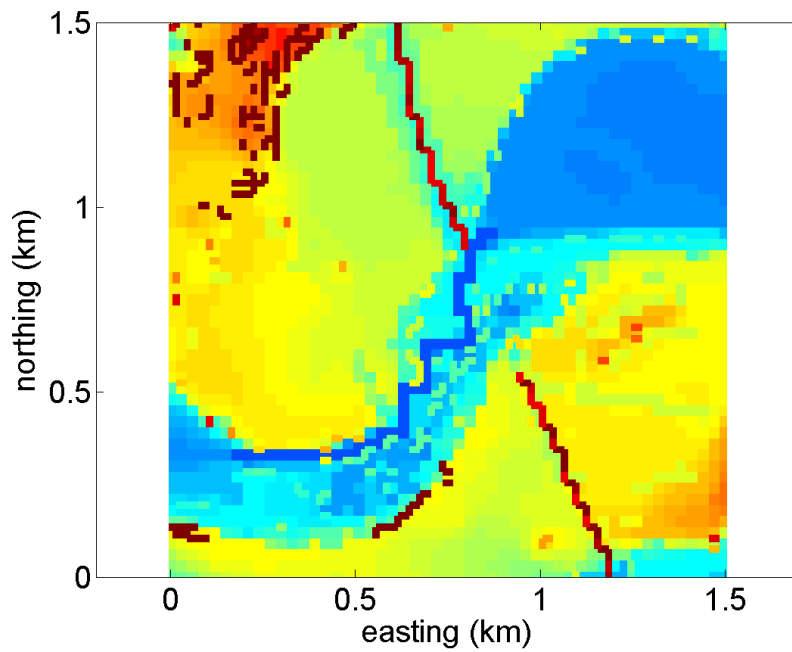
Figure 3: Sections of different Nueces DEMs processed from (a) 1×1 m lidar, (b) 30×30 m resolution with channels and edge blocking, and (c) a 30 median filter [White and Hodges, 2005]. Of particular note are the smaller channels in the upper right of (a) and (b) that are entirely missing from (c), as well as the railroad dike (red line along lower left) that is a continuous line in (a), a connected edge feature in (b), and is entirely absent in (c).

(a) 1×1 m lidar data of bottom elevation for a 1.5×1.5 km section in Nueces Delta

(b) 30×30 m bathymetry data with channels and edge features for the same section

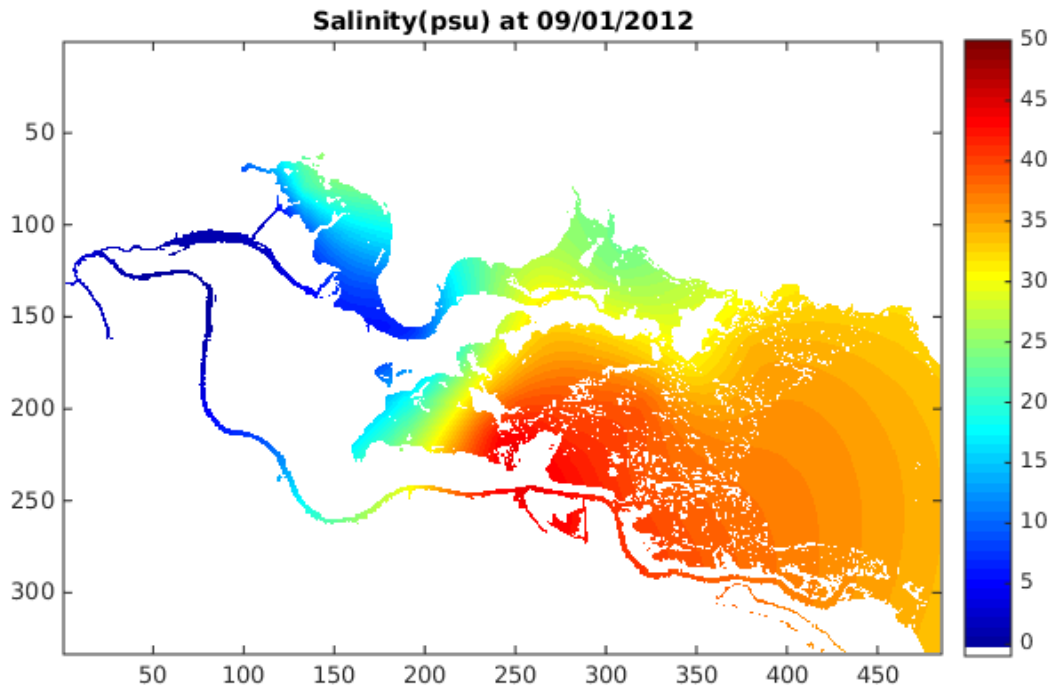Figure 4: Comparison of Lidar data and bathymetry used in NDHM (color scale is identical to Fig. 2).

Figure 5: Salinity field for initial conditions using kriging from the TWDB data.

2.3 Initial conditions

Initial conditions for any hydrodynamic model are a challenge. To start a model run, the water surface elevation, salinity, and velocities must be specified in every grid cell at the exact model start time. Clearly, such comprehensive synoptic data is impossible to obtain; so every model run begins with some error in the initial conditions. In a dynamic system, the error associated with the initial conditions will "wash out" of the system over time. That is, over time, the system will, in effect, forget the starting conditions and the model results will be driven by the boundary forcing conditions. The length of time it takes for the initial condition errors to become negligible is known as the "spin-up" time. One can think of this as the residence time of the initial condition error.

The velocity initial conditions for the NDHM can be set to zero without introducing substantial error. Velocities throughout the delta are relatively small and quickly respond to local water surface gradients and wind stress, so the spin-up time for the velocity is generally minutes to hours.

Initial conditions for salinity are the greatest challenge because the residence time of salt in the Nueces Delta can be weeks or months, depending on winds, tides, and inflows. Thus, effects of an incorrect initial salinity distribution can linger within the model simulations. We used a kriging approach for spatial interpolation from the field measurements at 14 TWDB salinity stations on Sept. 1, 2012. The initial salinity field is shown as Fig. 5

The water surface elevation is somewhat more troublesome than velocity, but not as sensitive as the

9

salinity. Ideally, a model should begin from a data set interpolated from field measurements, similar to the kriging used for salinity. In the present work, we took a simpler approach and applied a uniform (flat) free surface at the tidal elevation for the starting condition. A full evaluation of the effect on the free surface initial condition on spin-up time remains a subject for future investigation.

2.4 Boundary conditions

The evolving tidal elevation, salinity at the tidal boundary, wind speed, wind direction, and freshwater inflows are required boundary conditions for the model. The tidal boundary data were extracted from Station 185 records in the Texas Coastal Ocean Observation Network (TCOON). In the prior NDHM work, Ryan and Hodges [2011a] used tidal data from the White Point gage at the northern edge of Nueces Bay, but this station is no longer available in the TCOON network. Figure 6 shows the site locations in and near the study area. As we do not have any information on water surface gradients across the width of Nueces Bay, the tidal elevation is forced as a uniform value across the eastern model boundary. The salinity boundary condition for the tidal boundary of Nueces Bay was obtained from TCOON Station 074 (SALT03). Wind data was from TCOON Station 069 (Nueces Delta Weather Station). Freshwater pumping boundary conditions for calibration and validation simulations (§3, 4) were obtained from the Nueces River Authority[1]. To evaluate pumping effects the freshwater inflows were set at fixed values discussed in §5.
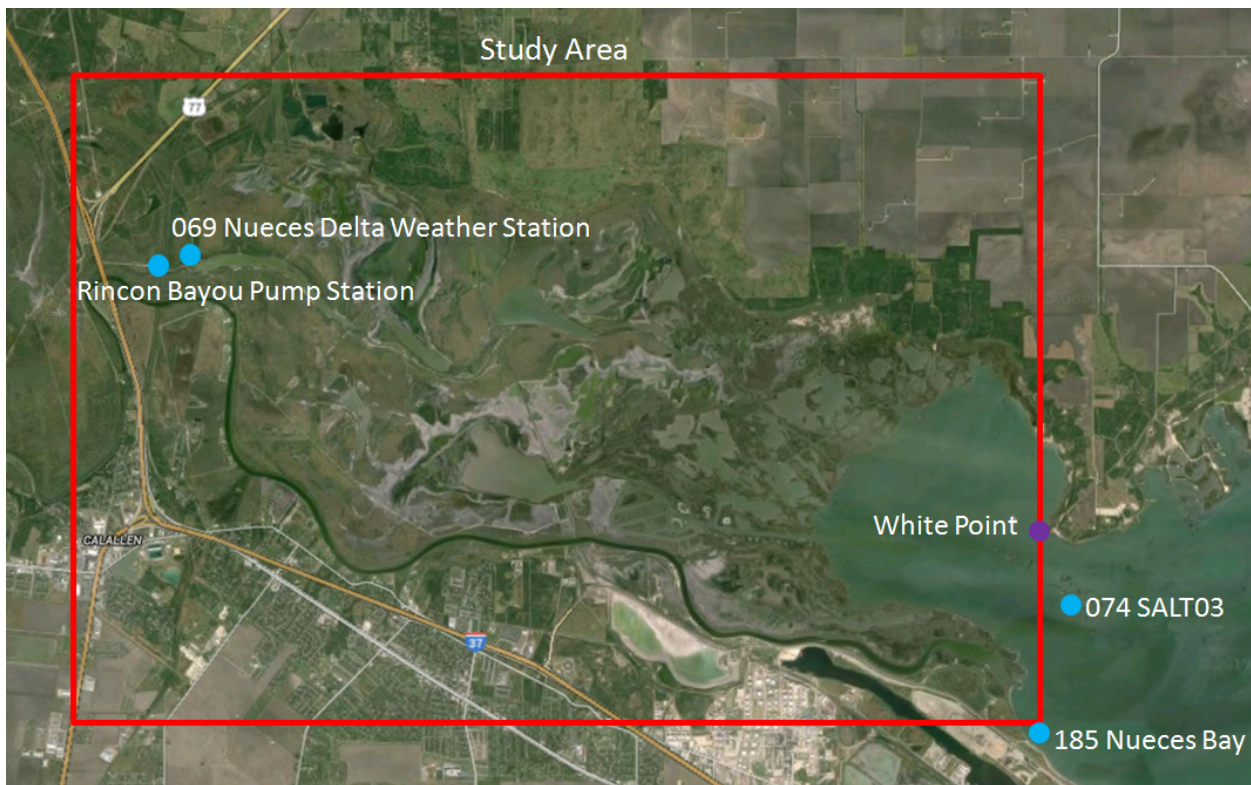

Figure 6: Locations of data stations for boundary conditions and the pump station where freshwater inflows are piped from upstream in the Nueces River (map from Google Earth). The red square is the modeled area of NDHM.

---

[1]http://www.nueces-ra.org/CP/CITY/rincon/ accessed 8/5/2015

3 Calibration of the NDHM

Calibration is often thought of as adjusting a model to "get the right answer," where the "right" answer is evaluated by comparison of model predictions and observations. A more realistic goal for calibration is to obtain a "better" model that shows less disagreement with observations. However, with any complex model, and particularly with a hydrodynamic model, care must be taken to ensure that the calibration process does not get the right answer (or even a better answer) for the wrong reasons. A hydrodynamic model is subject to a number of error sources from its initial conditions, boundary conditions, and numerical algorithms, but calibration is typically only compensating for a single error source. For example, calibration for hydrodynamic models is usually accomplished through adjustment of drag or roughness coefficients (C_D or Manning's n), so that flow is slowed or accelerated to better match observed water surface elevations and velocities. This calibration approach is well-founded if the principal source of error is in the unknown roughness and turbulence effects. However, if the model error is being driven by another source (e.g. spatial variability in the wind, Laval et al. [2003]), then adjusting the roughness is actually a distortion of the physics that makes the model less reliable. That is, there is no reason to believe that a model is a "better" representation of the flows *throughout* the domain simply because the error is reduced at a few observation points. Thus, the first question to ask is: *how sensitive is my model error to global changes in my calibration parameter?* If the error is relatively insensitive to the calibration parameter, then it is questionable as to whether detailed calibration adjustments with that parameter can create a better model.

Within the Frehd code that underlies the NDHM, the only direct calibration parameters are the bottom drag coefficient and the wind drag coefficient. The former affects the rate of energy dissipation by the water, and the latter affects the rate at which wind transfers momentum to the water. To date, we have only worked on calibration using the bottom drag coefficient. Note that the concepts of "drag" and "roughness" refer to the same phenomena, but usually have slightly different algorithms. The Frehd model uses drag coefficients where the total drag force (F_D) is a grid cell is related to the flow velocity (V)

$$F_D = \frac{1}{2} C_D \rho V^2 \Delta x^2 \tag{1}$$

where ρ is the water density and Δx is the grid size. The drag coefficient can be related to Mannings n, the water depth (d) and gravity (g) by

$$C_D = g \frac{n^2}{d^{1/3}} \tag{2}$$

as discussed by Pasternack et al. [2006][2].

Traditionally, roughness is thought of as small-scale bed features and vegetation that affect the turbulent boundary layer in a fluid flow; increased roughness causes increased energy dissipation and leads to lower velocities. However, roughness in the NDHM must also include the effects of subgrid-scale features that are neglected at the scale of the model grid, i.e. the effects of the 900 subgrid features that are averaged from the 1×1 m DEM to create the 30×30 m NDHM grid. We have partially addressed this problem through the development of blocking edges and channelization (see §2.2 above), but non-blocking and non-channelization
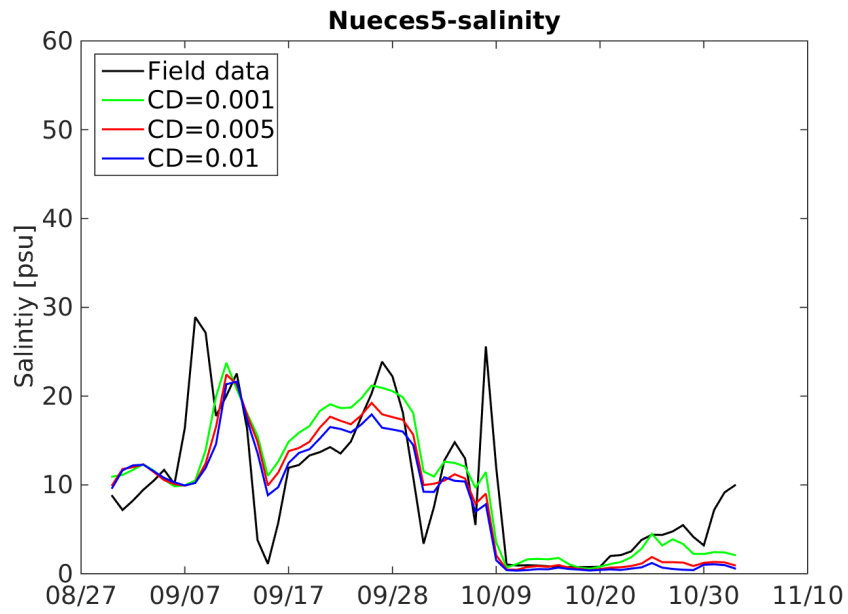
---

[2]Note that Pasternack et al (2006) cites an out-of-print technical report (US Department of Transportation FHWA-RD 88-177) for the equation relating C_D and n. However it is not clear whether that document originated the idea, or if it is found in prior technical reports.

topographic features that are smaller than the grid resolution are still neglected in the present model. Furthermore, the NDHM presents a complex problem as the channel connectivity through the delta at the 30 m grid scale was obtained by increasing the width of small channels in the fine-scale DEM (§2.2). It is not clear what roughness values should be applied these small channels to counteract the artificial widening. Finding physics-based approaches to solving these problems is at the cutting edge of research, and is not addressed herein.

Our calibration approach was to analyze the model results for global changes in the drag coefficient using values of 0.01, 0.005 and 0.001 throughout the domain. We recognize that the vegetated areas above the typical tidal excursion should have higher drag coefficient than the channels, which was the approach for the original NDHM in Ryan and Hodges [2011a]. However, for simplicity in the calibration tests we used the same drag coefficient throughout the domain. Because the majority of the fluxes are carried through the channels, this simplification does not significantly alter the overall structure of the flow field.

The model results for the three tested drag coefficients have been compared with the field data collected the field observation stations shown in Fig. 2, above. The key point (from a calibration perspective) is illustrated in a subset of results presented in Figs. 7 and 8. Changing in the bottom drag coefficient has relatively minor impact on the difference between the observed and modeled values, and does not affect the larger error signals in the results. Thus, we do not see any justification for using the field data for detailed spatial adjustment of the drag coefficient. A global uniform bottom drag coefficient of 0.005 was adopted. Our conclusion is that the bottom drag coefficient is not the principal control on the flow structure in the delta. This result is consistent with the fluxes being primarily controlled by topographic connectivity, which is not surprising for the relatively low-velocity flows through the marshes and bayous.

As discussed further in §4 below, the differences between the modeled and observed salinities *cannot* be compensated through calibration of the drag coefficient. The salinity transport model is presently missing critical sources and sinks that affect the salt concentration (i.e. exchange with porewaters and evaporation), so any calibration that improved the salinity results would inherently be of questionable validity.
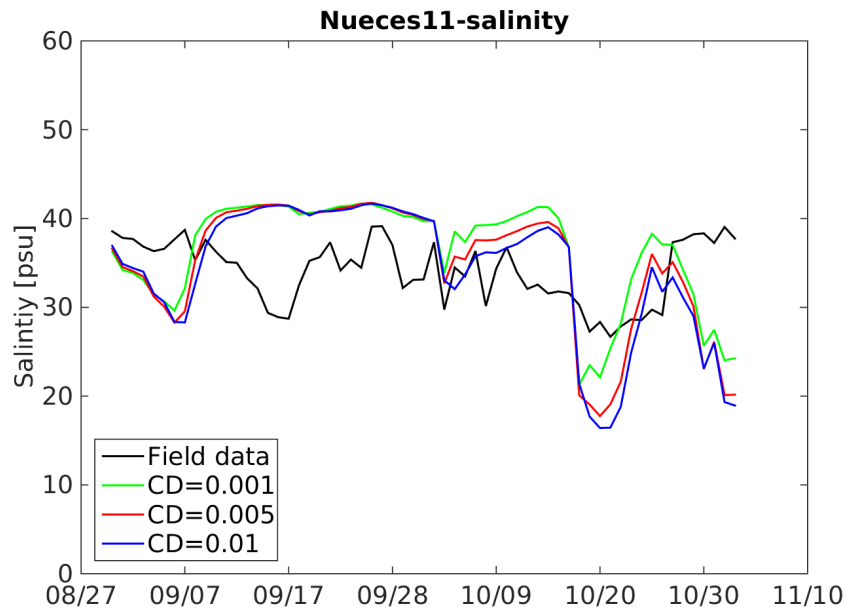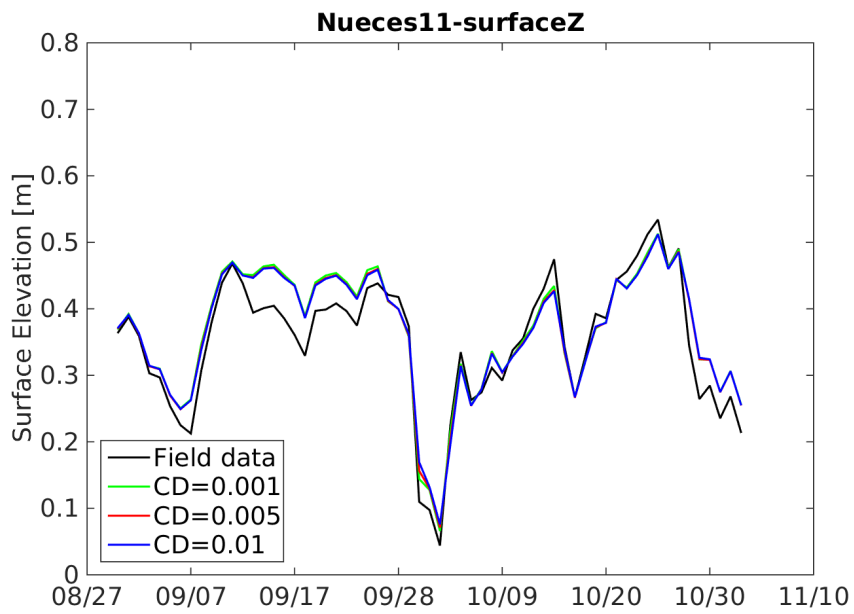
(a) Salinity

(b) Surface Elevation

Figure 7: Effects of different bottom drag coefficients at observation station Nueces5.

(a) Salinity

(b) Surface Elevation

Figure 8: Effects of Different Bottom Drag Coefficients at Nueces 11.

4   Validation of the NDHM

Formally, model "validation" requires comparison of model results to an observation data set that was not used for calibration. However, since the calibration results for the NDHM (§3, above) were relatively insensitive to the choice of calibration parameter, the full comparison between model results and observations can be considered a validation exercise.

The NDHM results were compared with the field data at the 14 observation stations from September, 2012 through July, 2013. Figures 9 through 22 show the daily averaged values for salinity and surface elevation (surfaceZ) at each station. We use the daily averages to remove the higher frequency tidal oscillations from the data.

A common thread through all of the results is that the NDHM is much better at capturing the water surface elevation than salinity. This result is not surprising as the error in the salinity is integrative of salt advection and depends on the cumulative salt flux through the channels. The salinity error is concentrated at the front between fresh and saltwater and can only be ameliorated by movement or exchange at the front. In contrast, the water surface elevation moves as a barotropic wave, whose effects can spread more quickly and thus dissipate local errors across the entire flooded domain. Furthermore, the NDHM does not include evaporation or salt exchange (storage/release) in porewaters of the sediments. Over the course of a year, we can expect these processes to have significant impacts on the salinity. Despite these issues, through comparisons of the field and model data we are able to identify some of the key issues and sources of error in the NDHM.

Figure 9 shows results for location Nueces1, which is close to the Rincon pipeline inflow at the upper end of the Rincon Bayou, The modeled surface elevation shows good agreement, with the exception of some of the larger spikes of short duration. The salinity in the model is significantly lower than the observed values throughout. We believe this discrepancy is due to two causes. First, the NDHM used for these tests does not include the connection of the Rincon channel to the main stem of the Nueces River. This channel is gated, but we did not have data on the operation of the gate during the field study so it was set closed throughout the study period. Salt water can move from the river to the upper Rincon Bayou when the gate is open, so this is a possible source of salinity at Nueces1. The second possible source of higher salinity is through upstream transport of high concentrations developed through evaporation in the northern tidal flats. This issue is discussed further below with results from Nueces2, Nueces3, and Nueces7.

Figure 10 shows results for location Nueces2, which is at the junction of the Rincon Bayou and the overflow channel. Again, the surface elevation results appear reasonable, although there are several larger excursions in the observations that are not matched in the model. The salinity in the model underestimates some of the same features seen at Nueces1 in Fig. 9. In particular, there is a strong increase in salinity from March through June with peak values over 55 psu, which is also seen at downstream stations Nueces3, Nueces4, and Nueces6; see Figs. 11, 12 and 14, below. However, further downstream the locations Nueces7 and Nueces10 (Figs. 15 and 18) do *not* show salinities over 45 psu. Thus, the higher salinities in the upper tidal flats of Nueces3 and Nueces4 are not caused by upstream tidal/wind salinity transport, but must be associated with evaporation and/or porewater salt release. As these processes are not included in the NDHM, it is not surprising that the high salinity conditions are consistently underestimated in the model.

Locations Nueces3, Nueces4, and Nueces5 (Figs. 11 – 13) are in relatively close proximity at the edges

or within the northwest tidal flats. This area is a challenge for the model as the water depths appear to be controlled by some relatively fine-scale features that are not well represented in the model (e.g. sediment bars that have accumulated near the mouth of the Rincon overflow). Nueces5 appears to get the overall surface elevation correct, with the exception that it dramatically undershoots the observations during the winter. This same undershoot is seen in the surface elevation at Nueces6 (Fig. 14), but not at Nueces7 or Nueces10 (Figs. 15, 18). Indeed at these further downstream sites it can be seen that the observed water surface elevation shows the lower values that occur in the model at the upstream stations. Because this error is first seen at Nueces6 (Fig. 14), it is likely that the cause is the model bathymetry representation of the narrow channel under the railroad bridge in the lower Rincon Bayou, i.e. the section illustrated in Fig. 4, above. The deeper excursions of the water levels over the winter at Nueces5 and Nueces6 is consistent with a wider channel that allows water to rapidly exit the middle Rincon Bayou.

Salinities at locations Nueces6, Nueces7, and Nueces10 (Figs. 14, 15, 18) provide insight into the effects of upstream salinity (evaporation or porewater salt release). At the furthest downstream location, Nueces10, the model salinity is a reasonable proxy for the observed data, mostly showing excursions of similar sizes and timing. In contrast, moving upstream to Nueces7 and Nueces6, we see the observed salinity taking on a bias such that it is always larger than the model, with the effects being greater further upstream. These features are consistent with an upstream increase in salinity through evaporation and/or porewater salt release.

Figure 16 shows results for location Nueces8 located in the northern tidal marshes. We are still unsure about the interpretation of these results, and further investigation is necessary. The relatively flat surface elevation through much of the year could be interpreted as either a thin layer of water (i.e. negligible depth) or a ponded region. In either case, we would expect the salinity to remain relatively constant when there is little change in the surface elevation. However, within the salinity model results, the periods with the constant water level are indistinguishable from the periods with a changing water level. We are investigating whether there is a latent bug in the code, or if there is some other explanation for this behavior.

Figures 17 and 19 show results for locations Nueces9 and Nueces11 in the saltwater tidal marshes away from the main channels. The water surface elevations are modeled quite well, which is not surprising as these are dominated by the tidal elevation in Nueces Bay. The salinity captures the general trends at Nueces9, but misses salinities higher than 40 psu at Nueces11. We speculate that the higher observed salinities at Nueces11 might be associated with porewater salinity release.
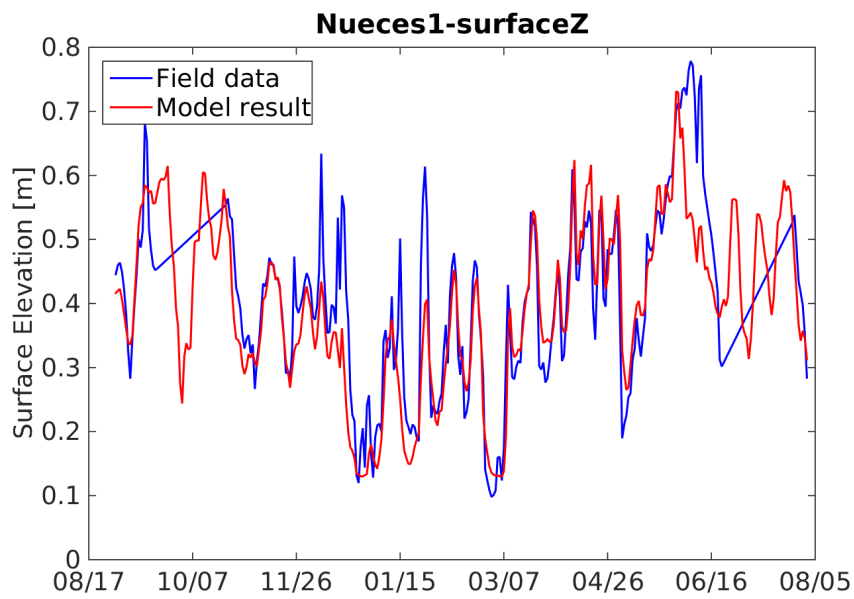
Figures 20 – 22 show results for Nueces12, Nueces13, and Nueces14, which are along the channel supplying/draining South Lake. The surface elevation results at the upstream Nueces12 and midstream Nueces13 have good agreement, although the minimum modeled surface elevation at Nueces13 appears to be significantly higher than the observations. This result could indicate a ponding effect or model bottom elevation that is higher than where the sensor was mounted. The surface elevation at Nueces14 (closer to NuecesBay), is dramatically different than the observations, and is the poorest agreement of the water surface elevation results. We suspect that the surveyed elevation of the Nueces14 sensor may not match the model datum. This hypothesis is supported by comparison of the Nueces13 with the Nueces14 results. It can be seen that the modeled surface elevations at Nueces13 and 14 are almost identical at the peaks, with the Nueces13 (upstream) data not seeing the lower excursions. In contrast, the peak events at Nueces14 show surface elevations that are 0.2 m less than upstream at Nueces13. As these sensors are separated by only 2 km and are both on the same channel, the simplest explanation is a problem with the vertical datum rather than a dramatic drop in water level over a such a short distance.

The salinity at Nueces14 (Fig. 22) shows similar trends in observed and modeled with the exception of the period from October through January. It is not clear if these results are a delayed effect of spin-up (i.e., incorrect initial salinity from kriging, Fig. 5) or possibly porewater salinity release. The larger excursions of salinity seen at Nueces14 indicates a larger source of upstream salinity that is being removed as the secular tide drops the overall level of Nueces Bay during the winter. The bias towards high salinities at the upstream Nueces12 and Nueces13 provides further indication that either the initial salinity field in the South Lake area did not contain sufficiently high salinities, or higher salinities are being produced by evaporation and/or porewater salinity release.

Overall, the NDHM validation results are encouraging. The water surface elevations are modeled quite well and the salinities have reasonable agreement. Improving the salinity agreement will likely require including effects of evaporation and porewater salinity flushing to capture the higher salinities seen in the delta.
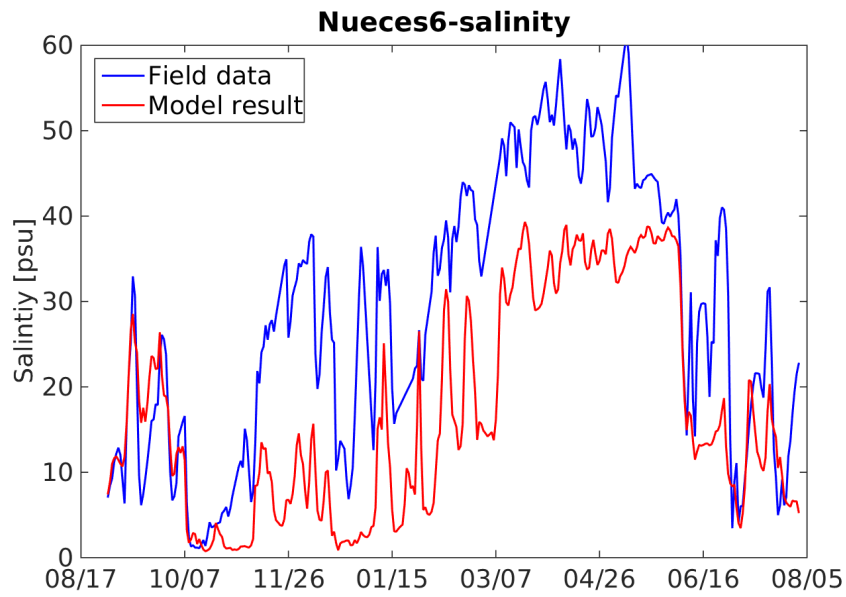
(a) Salinity

(b) Surface Elevation

Figure 9: Modeled and observed values for station Nueces1 at the upper end of the Rincon Bayou. Straight lines in the field data are a plotting artifact showing where instruments did not provide data.

(a) Salinity

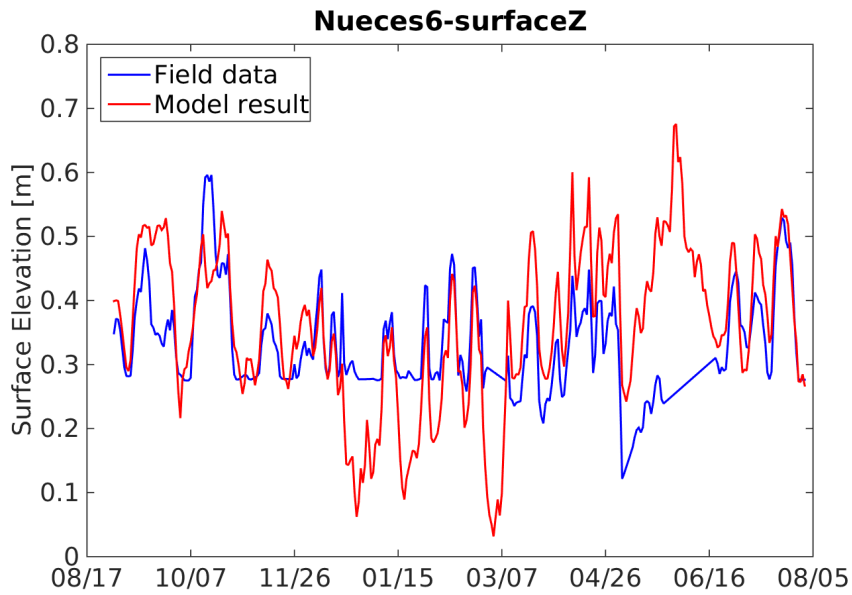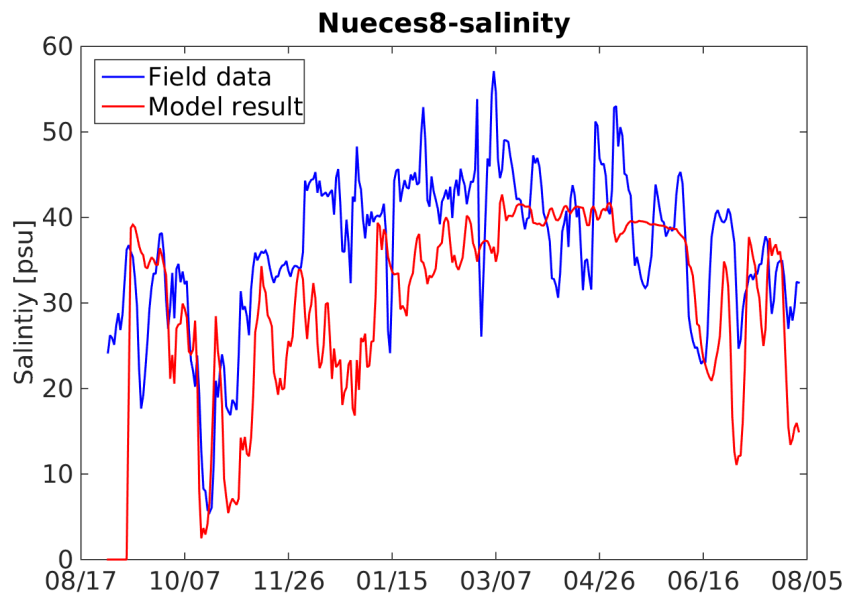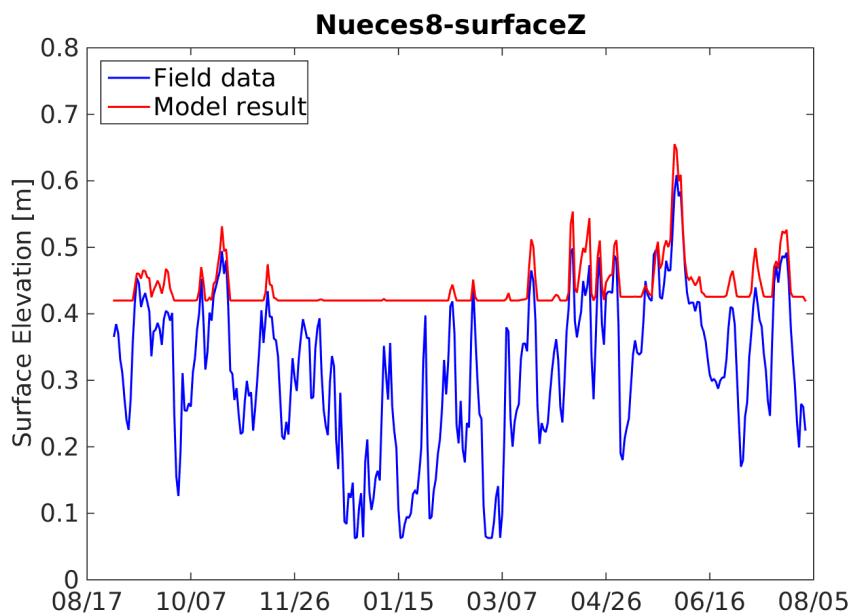(b) Surface Elevation

Figure 10: Modeled and observed values for station Nueces2 where the Rincon Bayou meets the overflow channel. Straight lines in the field data are a plotting artifact showing where instruments did not provide data.

19

(a) Salinity

(b) Surface Elevation

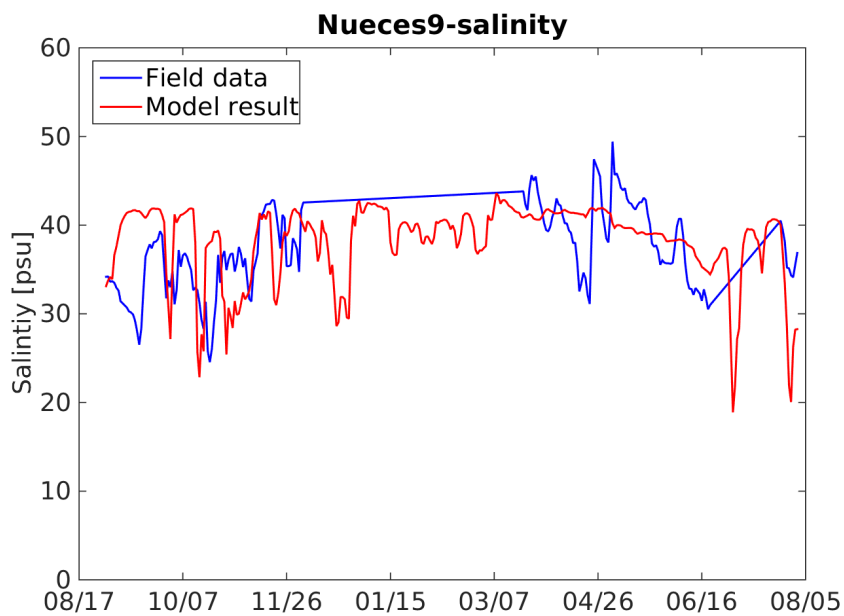Figure 11: Modeled and observed values for station Nueces3 at the mouth of Rincon overflow channel. Straight lines in the field data are a plotting artifact showing where instruments did not provide data.
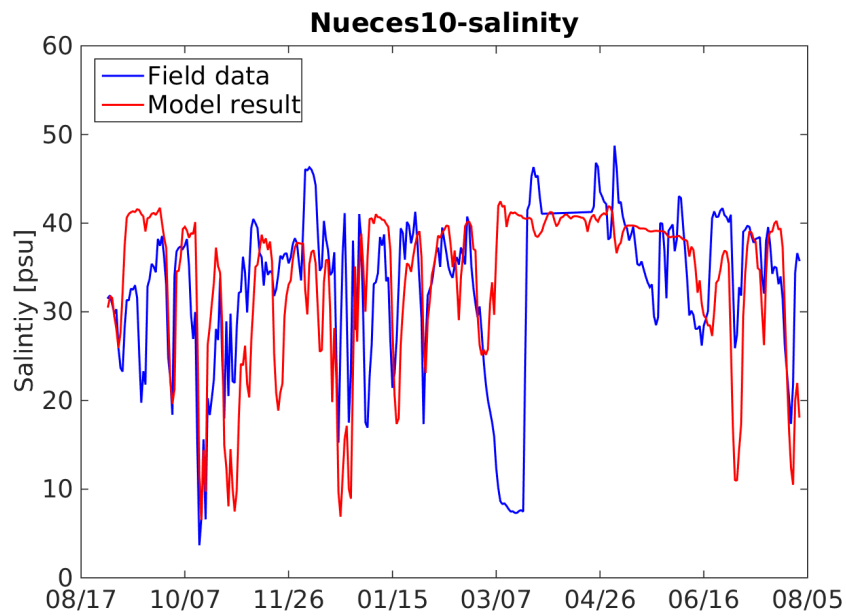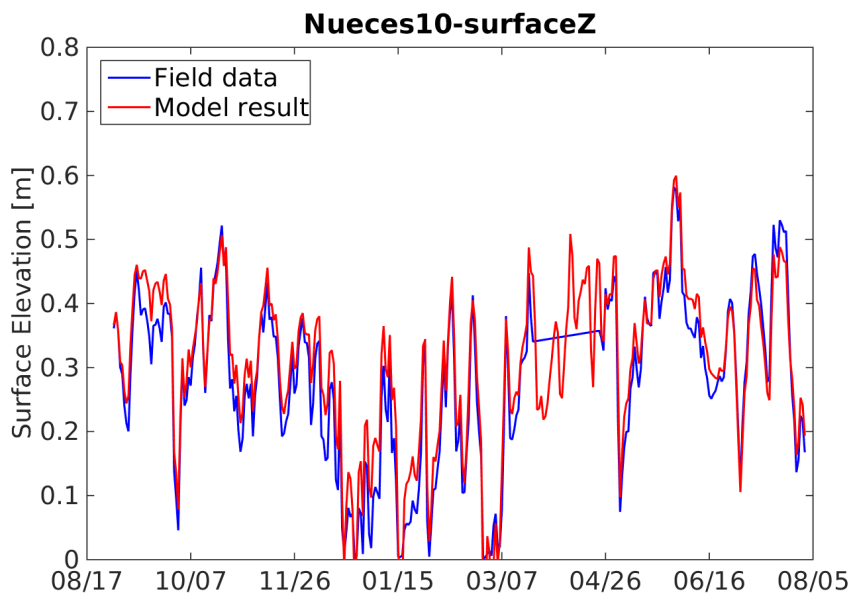
(a) Salinity

(b) Surface Elevation

Figure 12: Modeled and observed values for station Nueces4 within the northwest tidal flats. Straight lines in the field data are a plotting artifact showing where instruments did not provide data.
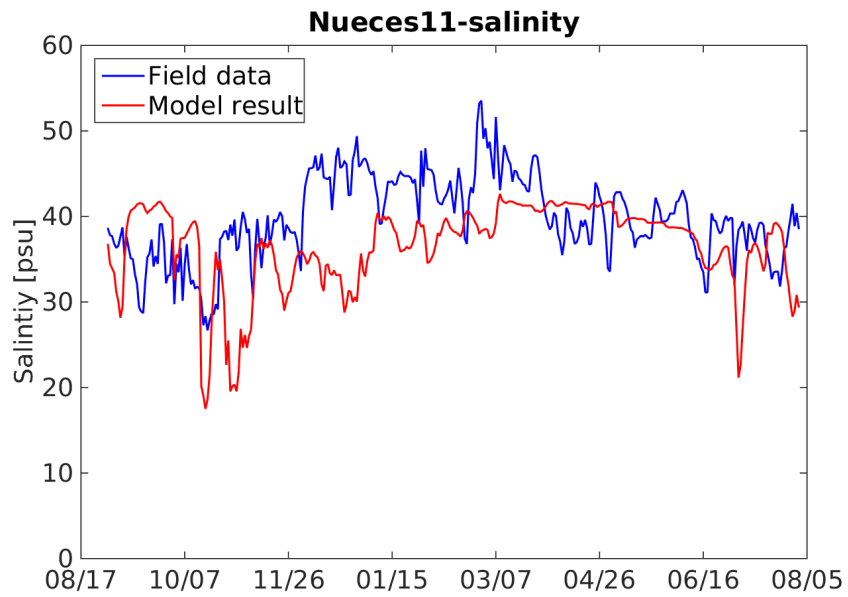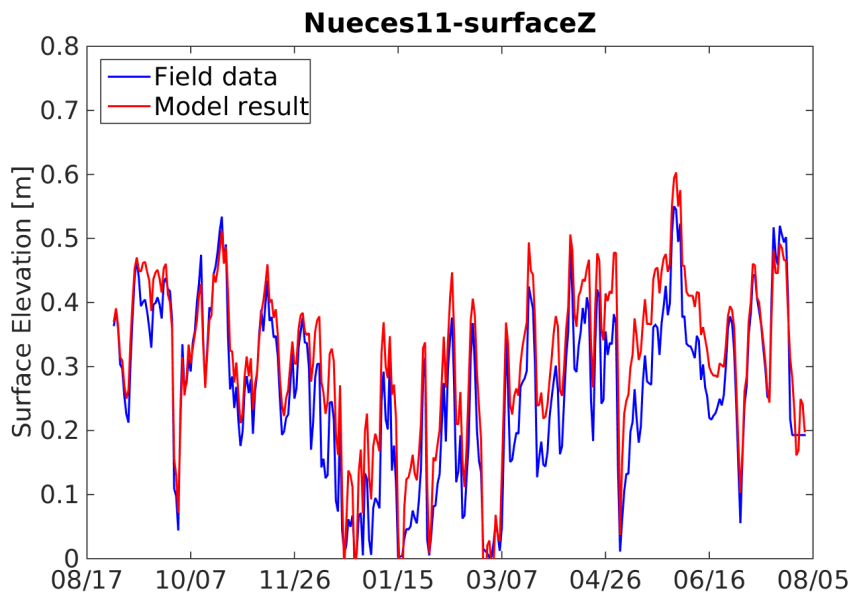
(a) Salinity

(b) Surface Elevation

Figure 13: Modeled and observed values for station Nueces5 where the upper Rincon connects to the middle Rincon and the tidal flats.

(a) Salinity

(b) Surface Elevation

Figure 14: Modeled and observed values for station Nueces6 in the middle Rincon just upstream of the railroad bridge. Straight lines in the field data are a plotting artifact showing where instruments did not provide data.

(a) Salinity

(b) Surface Elevation

Figure 15: Modeled and observed values for station Nueces7 at the downstream end of North Lake.

(a) Salinity

(b) Surface Elevation

Figure 16: Modeled and observed values for station Nueces8 in the northern tidal marshes.

(a) Salinity

(b) Surface Elevation

Figure 17: Modeled and observed values for station Nueces9 in the northeastern tidal marshes. Straight lines in the field data are a plotting artifact showing where instruments did not provide data.

(a) Salinity

(b) Surface Elevation

Figure 18: Modeled and observed values for station Nueces10 in the Rincon Bayou channel through the tidal marshes.
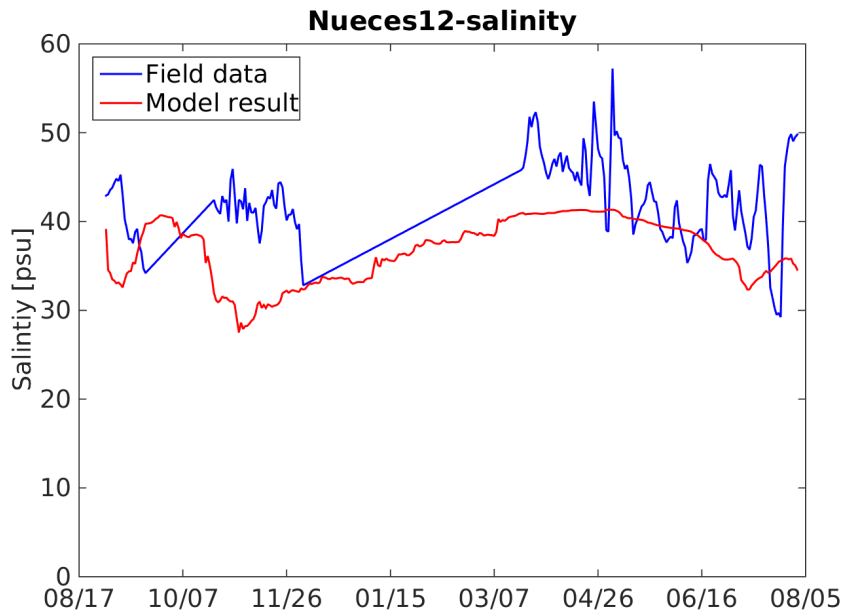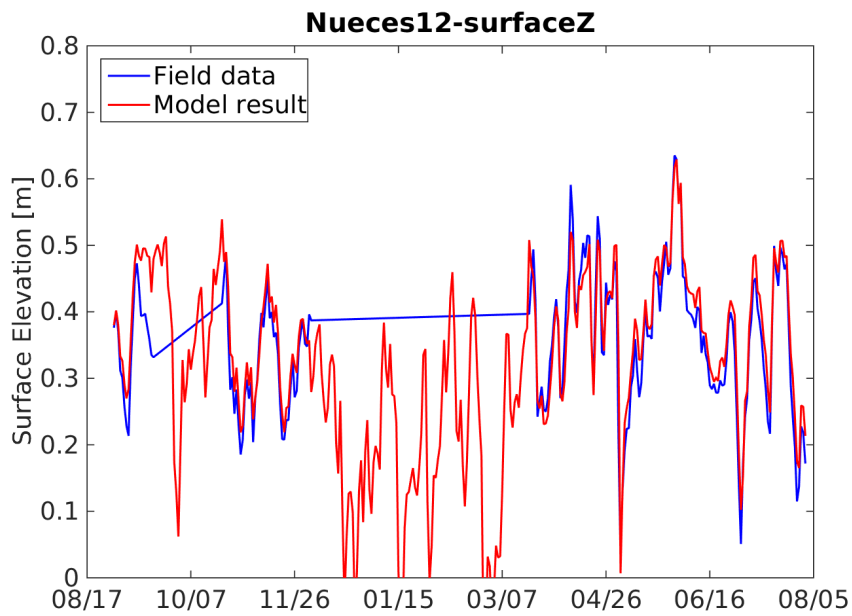
(a) Salinity

(b) Surface Elevation

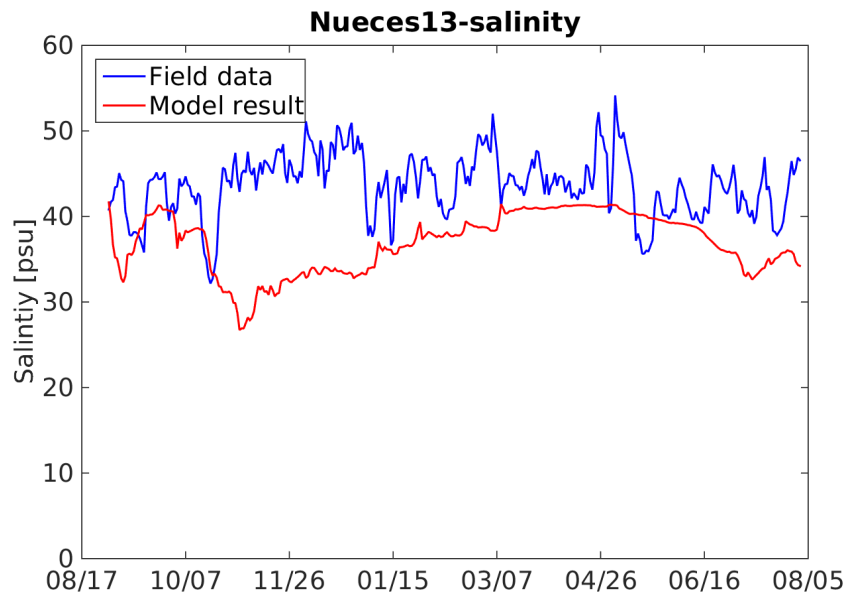Figure 19: Modeled and observed values for station Nueces11 in the central tidal marshes.
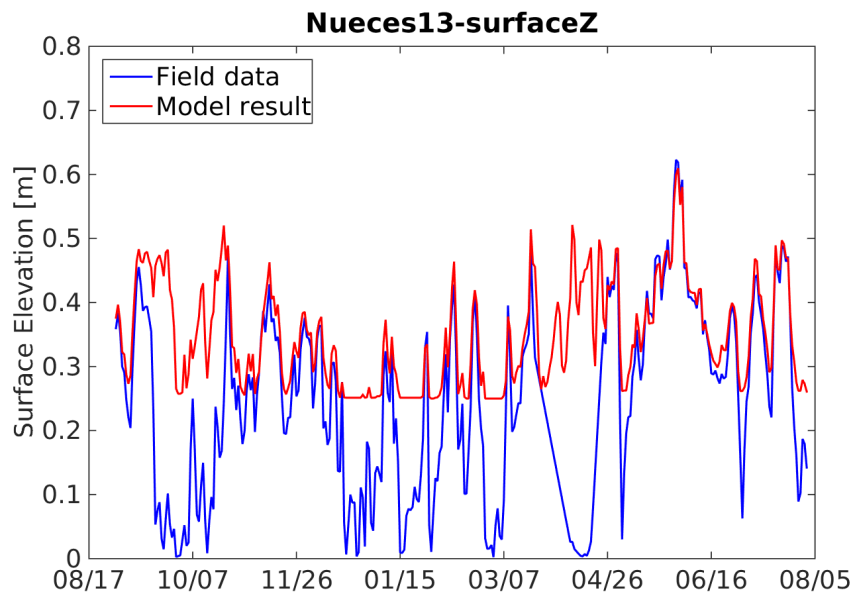
(a) Salinity

(b) Surface Elevation

Figure 20: Modeled and observed values for station Nueces12 at the outlet of South Lake. Straight lines in the field data are a plotting artifact showing where instruments did not provide data.
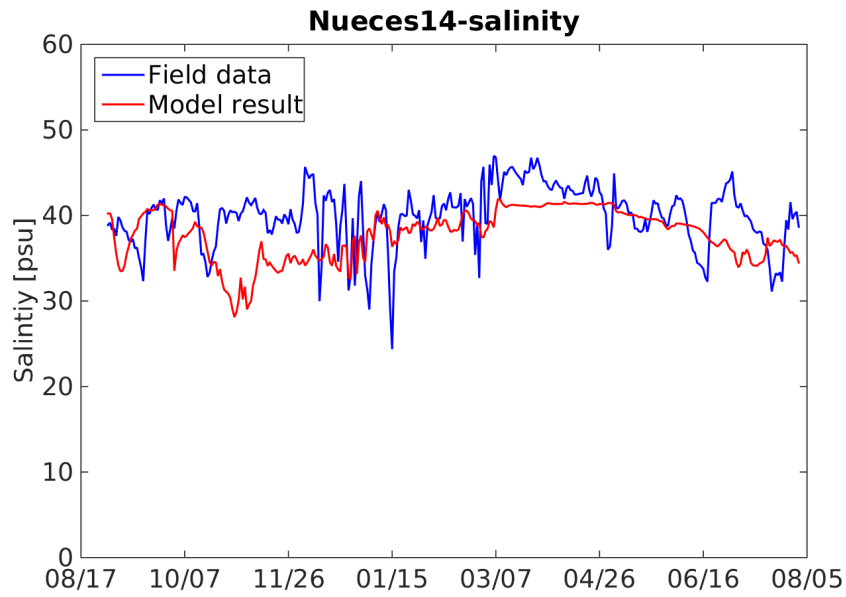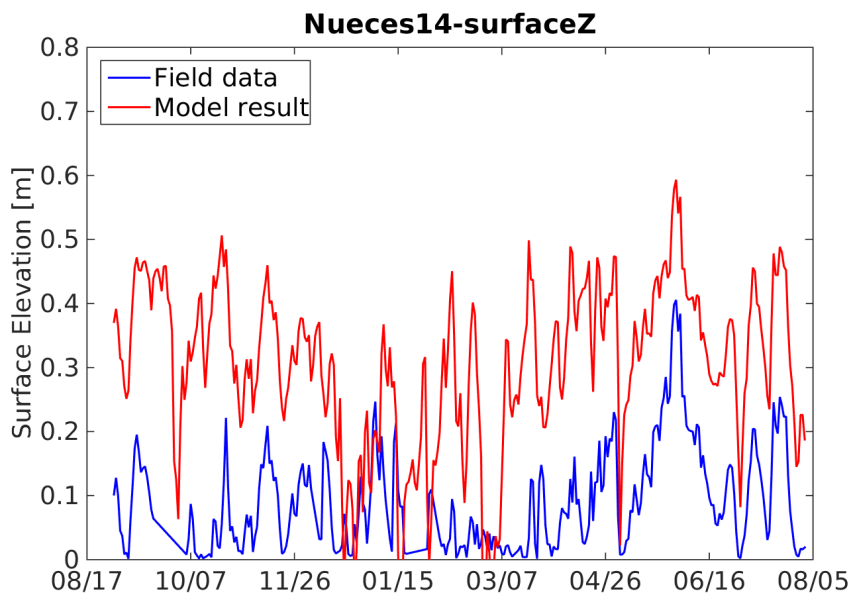
(a) Salinity

(b) Surface Elevation

Figure 21: Modeled and observed values for station Nueces13 upstream of the mitigation area.

(a) Salinity

(b) Surface Elevation

Figure 22: Modeled and observed values for station Nueces14 in the channel connecting the mitigation area to Nueces Bay.

5 Freshwater pumping scenarios

The exchange between freshwater and saltwater in the Nueces Delta is affected by winds and tide as well as the freshwater pumping rate. The Texas coast experiences a seasonal change in the overall tidal level – known as a secular tide – that typically results in lower tidal levels in months of January/February and June/July. These low periods are generally separated by higher levels from March through May and peak tidal elevations in September/October [Ward, 1997]. The wind patterns along the coast include sustained winds out of the southeast and frontal systems with winds from the north. Monthly averages for wind, tidal elevations, and wind directions (using TCOON data discussed in §2.4) for the Nueces Delta are shown in Tables 1 and 2. For each month we categorize the tidal elevation as either *Low* (less than 0.28 m), *Medium* (between 0.28 m and 0.33 m) or *High* (greater than 0.33 m). Wind speeds similarly can be categorized as *Slow* (less than 4 m/s) or *Fast* (greater than 4 m/s). Wind directions are categorized as predominantly southeasterly (*SE*), predominantly northerly (*N*) or transition (*Tr*) where there is not a dominant direction.

WIth three different tide categories, two different wind speed categories, and three wind direction categories there are 18 possible environmental forcing scenarios that can be combined with three possible pumping scenarios (1, 2 or 3 pumps) for a total of 54 cases. However, of the 18 possible environmental forcing scenarios, only 11 actually appear in Tables 1 and 2. Of those combinations that occur, we selected the six scenarios shown in Table 3 for investigation, and neglected combinations of *Low-Slow-SE, High-Slow-SE, High-Slow-N, Medium-Slow-Tr*, and *High-Slow-Tr.*

Each of the six scenarios in Table 3 were run with the three pumping scenarios for a total of 18 model cases. The Rincon Pipeline system is capable operating with 1, 2, or 3 pumps can provide 124, 203, or 265 ac-ft/day (respectively) of freshwater to the upper end of the Rincon Bayou [Lloyd et al., 2013]. Regardless of the number of pumps used in a scenario, the modeled pumping continued at the rated pump capacity for the first 10 days of the 30 day simulation and was then zero for the final 20 days. This corresponds to total freshwater supplies of 1240 ac-ft, 2030 ac-ft and 2650 ac-ft for the 1,2, and 3 pump cases, respectively.

Month	Tide	Tide	Wind Speed	Wind	Wind
	(m NAVD88)	Category	(m/s)	Category	Direction
2010-03	0.096	Low	4.26	Fast	SE
2010-04	0.291	Medium	4.86	Fast	SE
2010-05	0.357	High	N/A	N/A	SE
2010-06	0.335	High	N/A	N/A	SE
2010-07	0.490	High	N/A	N/A	SE
2010-08	0.290	Low	3.32	Slow	SE
2010-09	0.551	High	3.20	Slow	Tr
2010-10	0.321	Medium	2.99	Slow	Tr
2010-11	0.274	Medium	3.91	Slow	Tr
2010-12	0.126	Low	3.69	Slow	Tr
2011-01	0.149	Low	3.38	Slow	N
2011-02	0.059	Low	4.96	Fast	SE
2011-03	0.260	Medium	4.76	Fast	SE
2011-04	0.317	Medium	5.66	Fast	SE
2011-05	0.373	High	5.46	Fast	SE
2011-06	0.297	Medium	4.67	Fast	SE
2011-07	0.258	Medium	4.54	Fast	SE
2011-08	0.221	Low	4.32	Fast	SE
2011-09	0.238	Low	3.44	Slow	Tr
2011-10	0.280	Low	3.60	Slow	SE
2011-11	0.241	Low	4.34	Fast	SE
2011-12	0.238	Low	N/A	N/A	N
2012-01	0.076	Low	N/A	N/A	Tr
2012-02	0.203	Low	N/A	N/A	Tr
2012-03	0.293	Medium	4.80	Fast	SE

Table 1: Monthly averages for wind and tide, March 2010 through March 2012.

Month	Tide (m NAVD88)	Tide Category	Wind Speed (m/s)	Wind Category	Wind Direction
2012-04	0.363	High	N/A	N/A	SE
2012-05	0.330	Medium	4.26	Fast	SE
2012-06	0.399	High	4.07	Fast	SE
2012-07	0.331	High	3.99	Slow	SE
2012-08	0.313	Medium	N/A	N/A	SE
2012-09	0.349	High	N/A	N/A	Tr
2012-10	0.319	Medium	3.70	Slow	SE
2012-11	0.305	Medium	3.07	Slow	Tr
2012-12	0.197	Low	3.86	Slow	Tr
2013-01	0.153	Low	3.96	Slow	N
2013-02	0.215	Low	3.99	Slow	Tr
2013-03	0.218	Low	4.82	Fast	SE
2013-04	0.373	High	N/A	N/A	SE
2013-05	0.339	High	N/A	N/A	SE
2013-06	0.309	Medium	4.49	Fast	SE
2013-07	0.298	Medium	4.31	Fast	SE
2013-08	0.301	Medium	3.94	Slow	SE
2013-09	0.463	High	3.40	Slow	Tr
2013-10	0.459	High	3.52	Slow	SE
2013-11	0.444	High	3.53	Slow	N
2013-12	0.218	Low	3.22	Slow	N
2014-01	0.125	Low	3.32	Slow	Tr
2014-02	0.177	Low	3.97	Slow	Tr
2014-03	0.213	Low	4.25	Fast	SE
2014-04	0.315	Medium	4.60	Fast	SE
2014-05	0.332	High	4.70	Fast	SE
2014-06	0.371	High	5.28	Fast	SE
2014-07	0.203	Low	4.09	Fast	SE
2014-08	0.259	Medium	3.76	Slow	SE
2014-09	0.456	High	1.82	Slow	Tr
2014-10	0.389	High	3.23	Slow	Tr
2014-11	0.330	Medium	3.61	Slow	Tr
2014-12	0.292	Medium	3.19	Slow	Tr

Table 2: Monthly averages for wind and tide, April 2012 through December 2014.

Scenario	Tide	Wind Speed	Wind Direction	Occurrence	Data Used
1	High	Fast	SE	May, June	2014-06
2	Medium	Fast	SE	April, July	2014-04
3	Medium	Slow	SE	August	2014-08
4	Low	Fast	SE	March	2013-03
5	Low	Slow	N	January	2014-01
6	Low	Slow	Tran	December	2012-12

Table 3: Wind and tide scenarios used in model run. *Occurrence* is the typical months where these conditions are observed. *Data Used* is the year-month of the data applied as tide and wind boundary conditions.

Scenario	Case Tide/WS/WD	1 pump	2 pumps	3 pumps
1	H/F/SE	1640	2530	3088
2	M/F/SE	1475	2488	2880
3	M/S/SE	2021	2809	3248
4	L/F/SE	1795	2536	3106
5	L/S/N	1687	2495	2900
6	L/S/Tr	1898	2731	3283

Table 4: Inundation area coverage (acres) for different model runs.

Scenario	Case Tide/WS/WD	1 pump	2 pumps	3 pumps
1	H/F/SE	1.32	1.24	1.17
2	M/F/SE	1.19	1.23	1.09
3	M/S/SE	1.63	1.38	1.23
4	L/F/SE	1.45	1.25	1.17
5	L/S/N	1.36	1.23	1.09
6	L/S/Tr	1.53	1.34	1.24

Table 5: Inundation effectiveness (acre inundation / acre-ft pumped) for different model runs.

Figures 23 – 28 show the duration and area coverage over 30 days for freshwater inundation with different environmental scenarios and pumping schemes. Here "inundation" is defined as a minimum flooded duration of 6.2 hours, minimum depths of 1 cm, and maximum salinity of 15 ppt. Note that the coverage area for inundation is highly dependent on the selection of the minimum depth and maximum salinity allowable[3]. The overall inundation areas for these cases are provided in Table 4.

Figures 29 – 31 show the same results as Figures 23 – 28, but reorganized for visual comparison of different scenarios with the same freshwater pumping conditions.

The model results can be quantitatively compared across the different pumping scenarios by defining an "inundation effectiveness" as the ratio of the total area (acres) inundated by the total volume (ac-ft) provided by the pumps. This number provides the number of acres inundated by 1 ac-ft of water. The model results from Table 4 are presented in terms of inundation effectiveness in Table 5. It can be that in general, increasing the number of pumps decreases the inundation effectiveness, with the notable exception of the Scenario 2 (medium tide with fast wind from SE), where the 1 pump system is marginally less effective than the 2 pump system.

Our working hypothesis at the start of this project was that higher tides and strong winds from the southeast (Scenario 1) would maximize the inundation area (holding freshwater in the system with tides and wind) whereas lower tides with north winds (Scenario 5) would provide the minimum inundation area as freshwater is drawn down through the channels and pushed downstream by the wind. From Table 4, this clearly is not the case for the tested conditions. Indeed, it appears that the the medium tide with strong southeast winds (Scenario 3) provides the maximum area and effectiveness for 1 pump, with low tide combined with slow transitional winds (Scenario 6) as a close second place. The minimum (1 pump) effectiveness is a medium tide with fast southeasterly winds (Scenario 2), which we thought would be second only to Scenario 1.

However a qualitative review of the inundation maps does support some of the physical arguments in our original hypothesis. Comparing Fig. 27(a) that has north winds with Fig. 26(a) where the winds are out of the indicates that inundation duration in the upper delta is significantly reduced by the north wind, although the overall inundation area is not very different. Similarly, comparing the high tide in Fig. 23(a) with the low tide (similar wind conditions) of Fig. 26 shows that the higher tide does hold freshwater back, but in Scenario 1 this actually results in decreased inundation because the water is not able to reach the lower salt marshes where we would like the higher tide to help spread and retain the freshwater.

The present results must be used with caution as they do not appear consistent across changes in tidal elevation, wind speed, or wind direction. These results are not sufficient for definitive conclusions about the most effective environmental conditions for pumping. It seems likely that the complex interplay of wind, tide, and the delta topography during the inundation period are more important than the general tidal elevation level or wind direction.
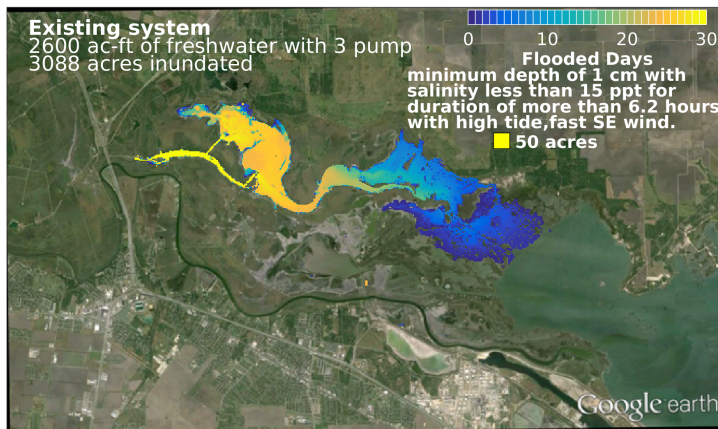
---

[3]pers. comm. Dr. Ken Dunton, UT Marine Science Institute. Note that Dr. Dunton recommended 25 ppt as a cutoff for computing inundation salinities rather than 15 ppt; however, the model validation in §4 shows significant and consistent underprediction of peak salinities, so we chose to use a more conservative lower cutoff for the present work.
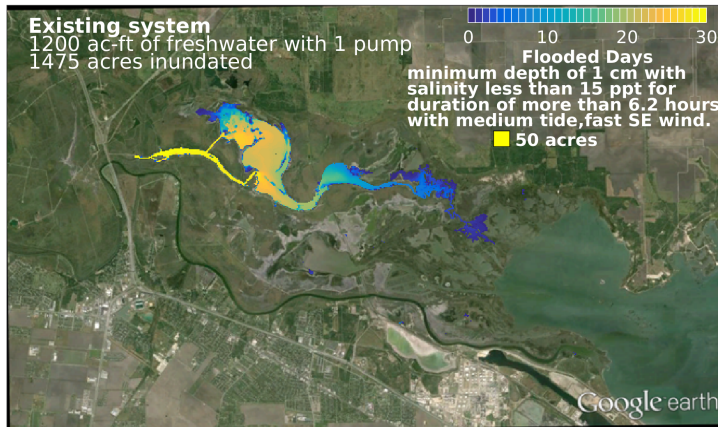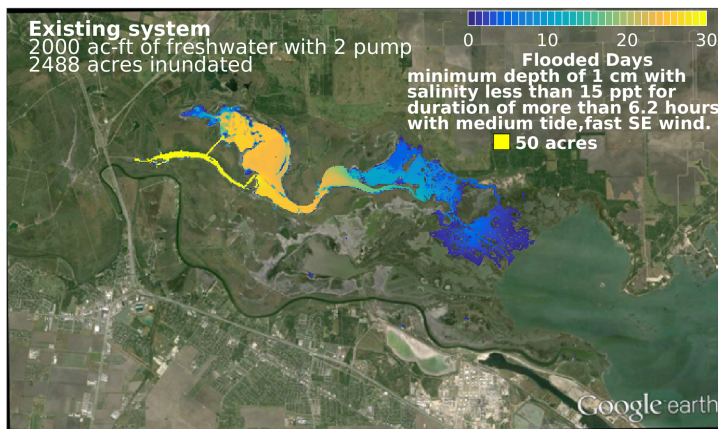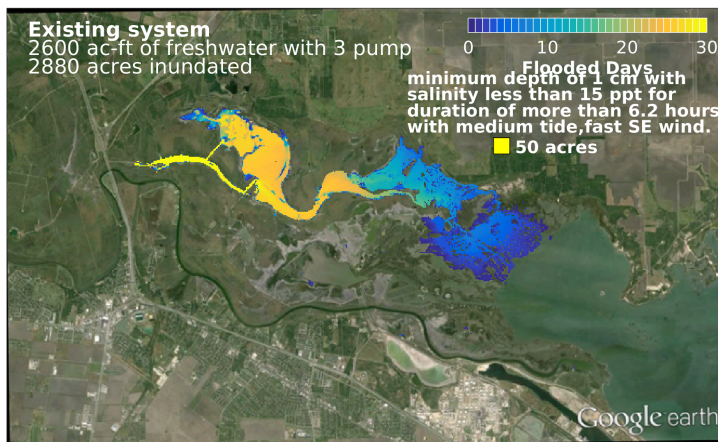
(a) 1 pump

(b) 2 pumps

(c) 3 pumps

Figure 23: Scenario 1: high tide, fast southeast wind. Colors indicate days flooded to depth greater than 1 cm with salinities less than 15 ppt for more than 6.2 hours.
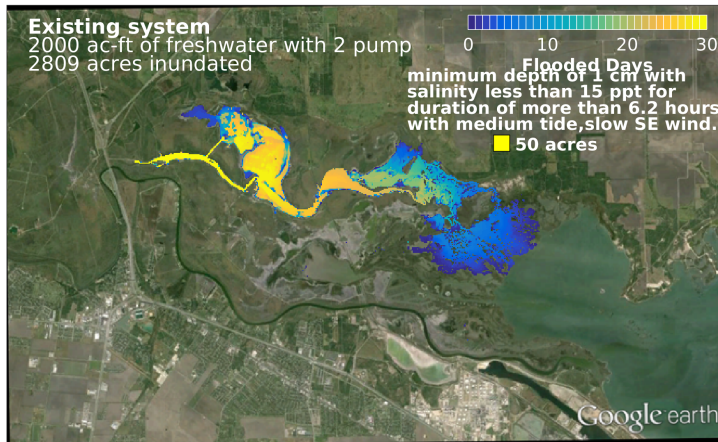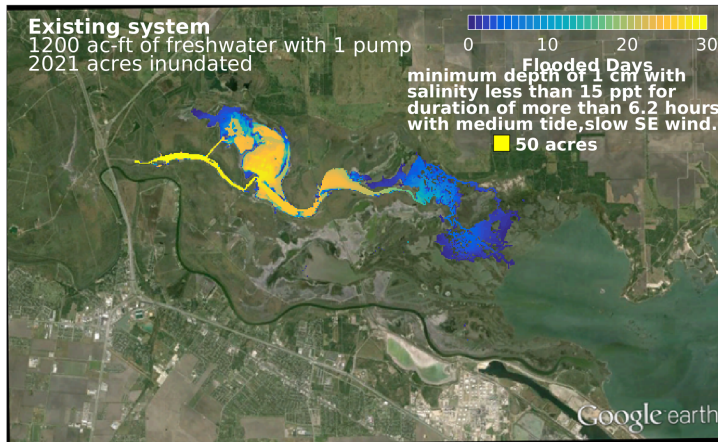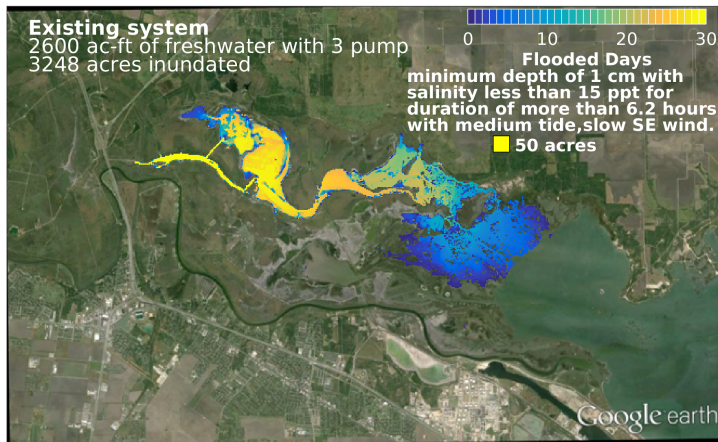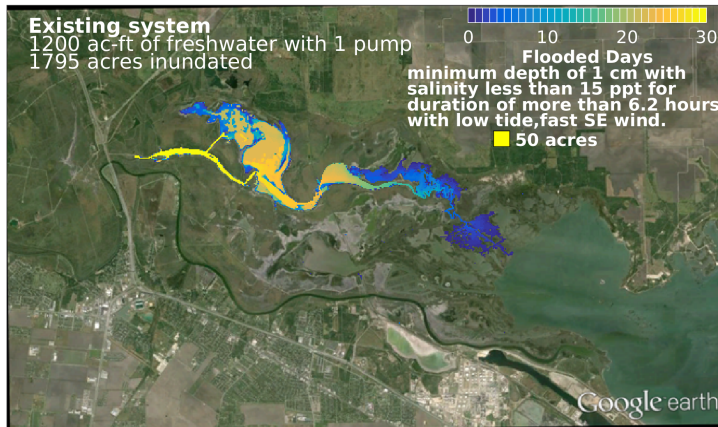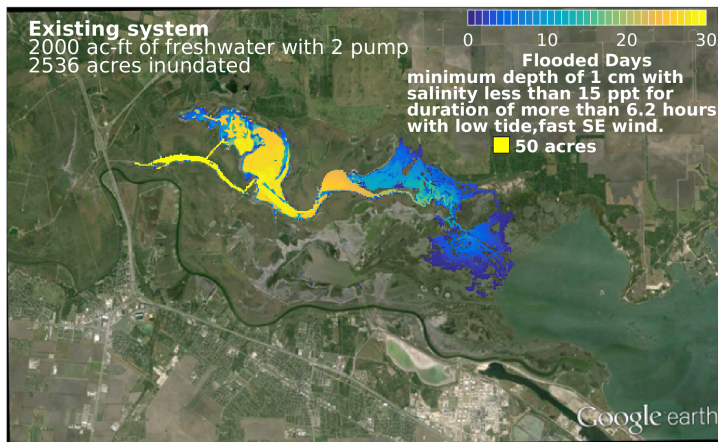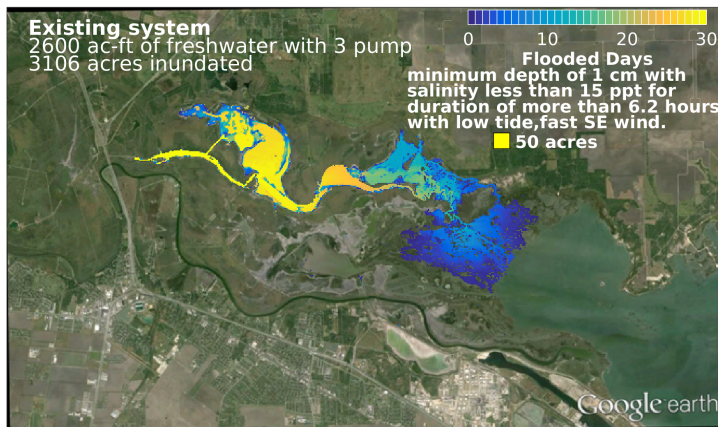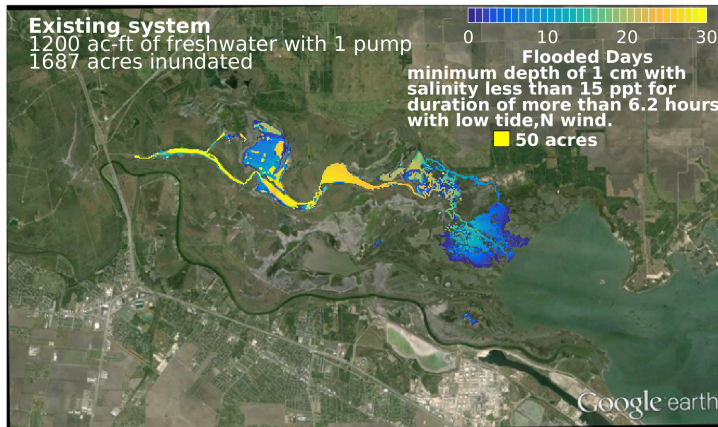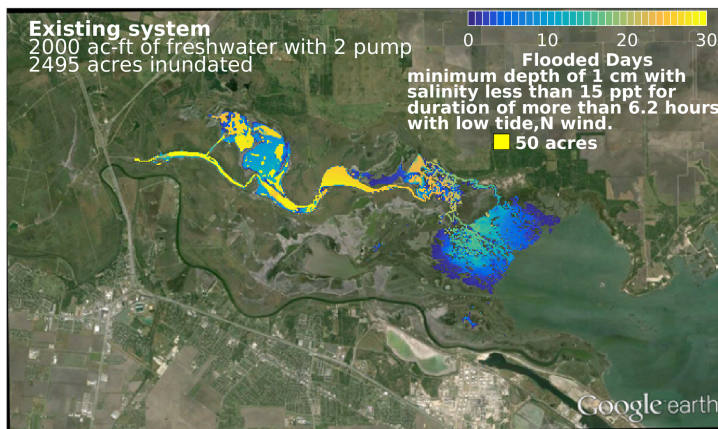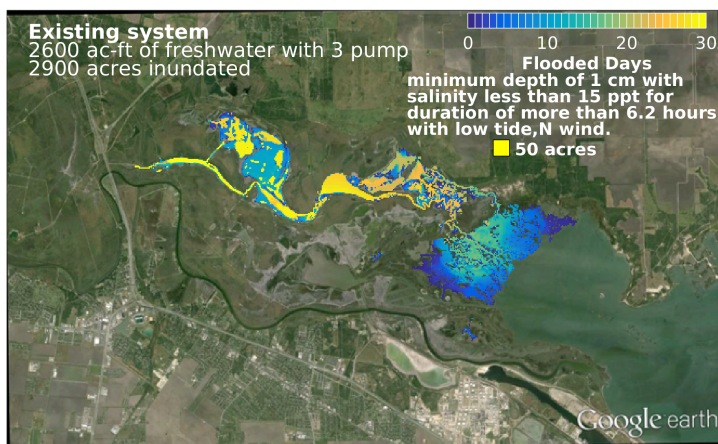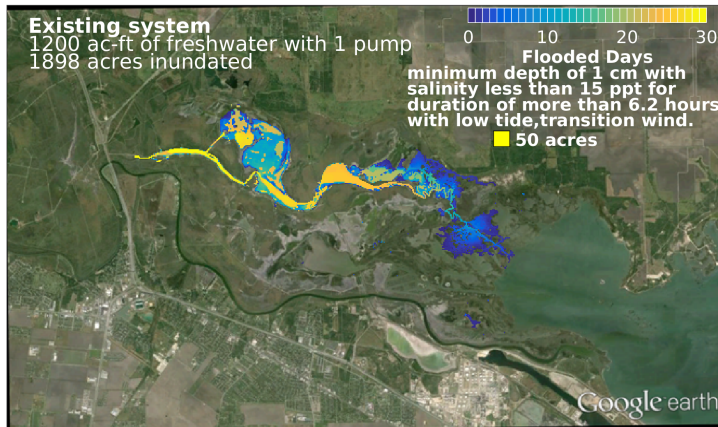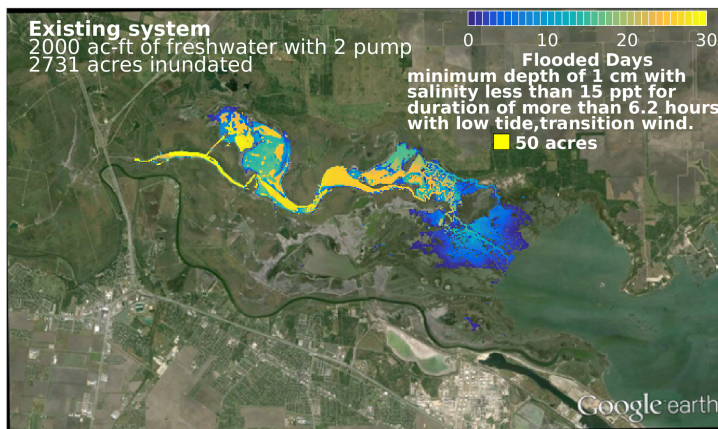
(a) 1 pump

(b) 2 pumps

(c) 3 pumps

Figure 24: Scenario 2: medium tide, fast southeast wind. Colors indicate days flooded to depth greater than 1 cm with salinities less than 15 ppt for more than 6.2 hours.

Existing system
1200 ac-ft of freshwater with 1 pump
2021 acres inundated

Existing system
2000 ac-ft of freshwater with 2 pump
2809 acres inundated

(b) 2 pumps

Existing system
2600 ac-ft of freshwater with 3 pump
3248 acres inundated

(c) 3 pumps

Figure 25: Scenario 3: medium tide, slow southeast wind. Colors indicate days flooded to depth greater than 1 cm with salinities less than 15 ppt for more than 6.2 hours.

(a) 1 pump

(b) 2 pumps

(c) 3 pumps

Figure 26: Scenario 4: low tide, fast southeast wind. Colors indicate days flooded to depth greater than 1 cm with salinities less than 15 ppt for more than 6.2 hours.
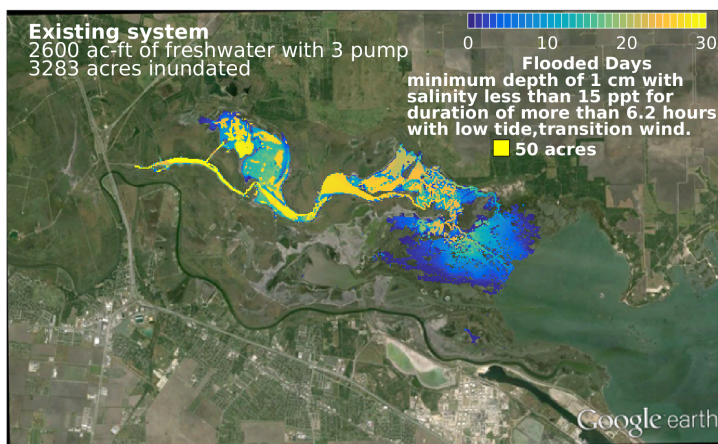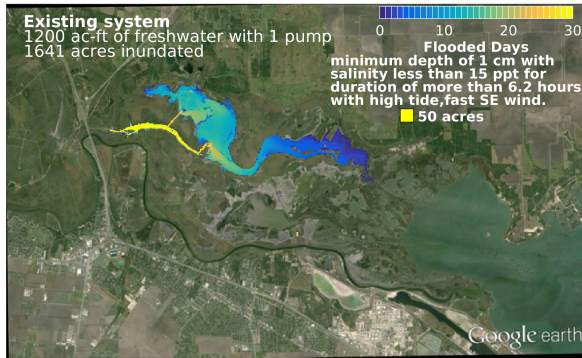
(a) 1 pump

(b) 2 pumps

(c) 3 pumps

Figure 27: Scenario 5: low tide, slow north wind. Colors indicate days flooded to depth greater than 1 cm with salinities less than 15 ppt for more than 6.2 hours.
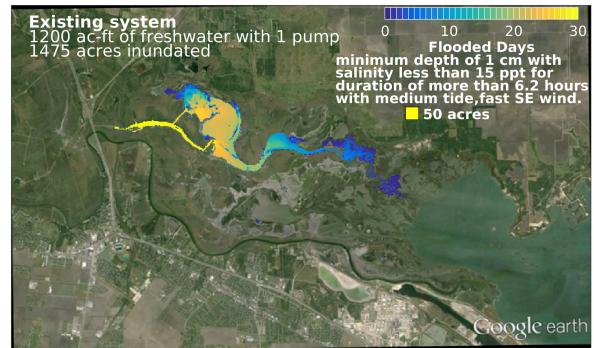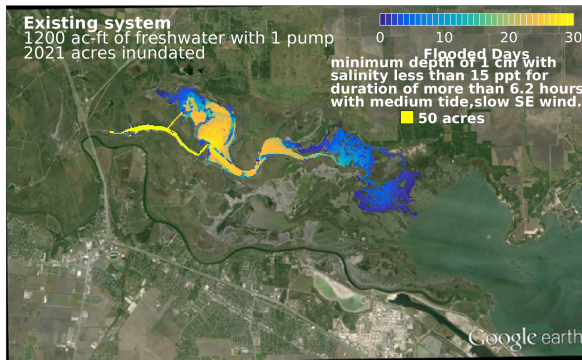
41

(a) 1 pump

(b) 2 pumps

(c) 3 pumps

Figure 28: Scenario 6: low tide, slow wind in transition. Colors indicate days flooded to depth greater than 1 cm with salinities less than 15 ppt for more than 6.2 hours.
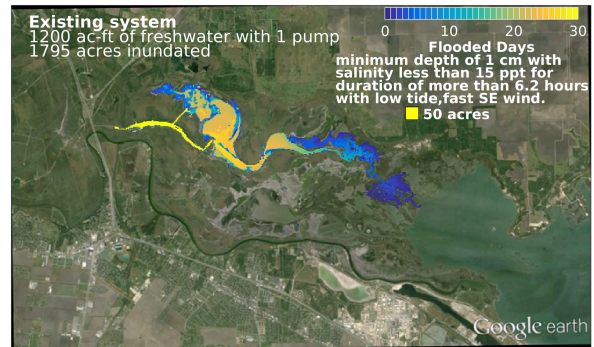
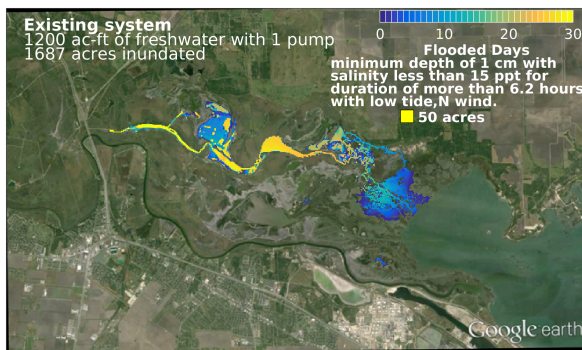(a) Scenario 1: high tide, fast southeast wind.

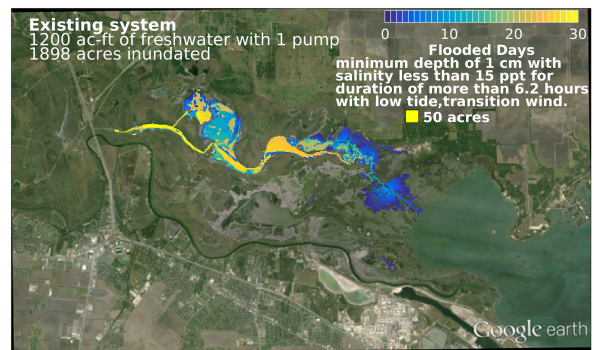(b) Scenario 2: medium tide, fast southeast wind.

(c) Scenario 3: medium tide, slow southeast wind.

(d) Scenario 4: low tide, fast southeast wind.

(e) Scenario 5: low tide, slow north wind.

(f) Scenario 6: low tide, slow wind in transition.

Figure 29: Comparison of 1-pump scenarios. Colors indicate days flooded to depth greater than 1 cm with salinities less than 15 ppt for more than 6.2 hours.

(a) Scenario 1: high tide, fast southeast wind.

(b) Scenario 2: medium tide, fast southeast wind.

(c) Scenario 3: medium tide, slow southeast wind.

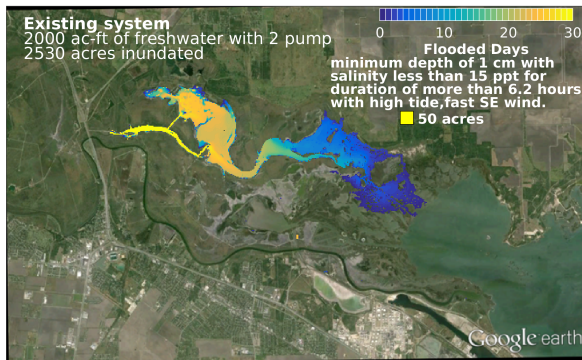(d) Scenario 4: low tide, fast southeast wind.
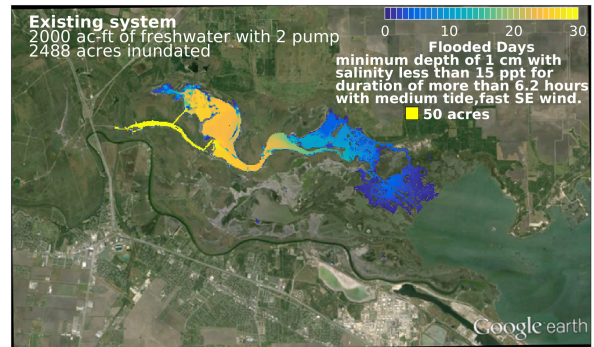

(e) Scenario 5: low tide, slow north wind.

(f) Scenario 6: low tide, slow wind in transition.

Figure 30: Comparison of 2-pump scenarios. Colors indicate days flooded to depth greater than 1 cm with salinities less than 15 ppt for more than 6.2 hours.

(a) Scenario 1: high tide, fast southeast wind.

(b) Scenario 2: medium tide, fast southeast wind.

(c) Scenario 3: medium tide, slow southeast wind.

(d) Scenario 4: low tide, fast southeast wind.

(e) Scenario 5: low tide, slow north wind.
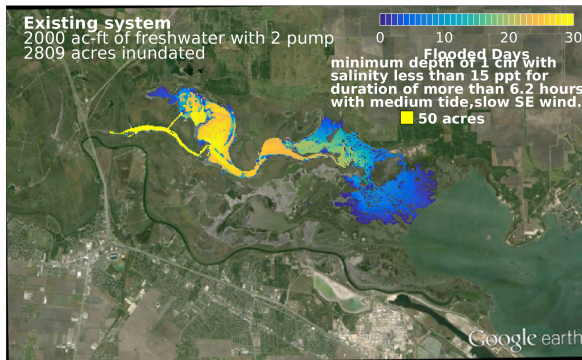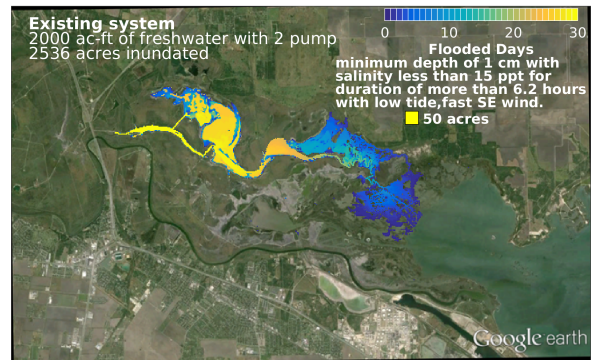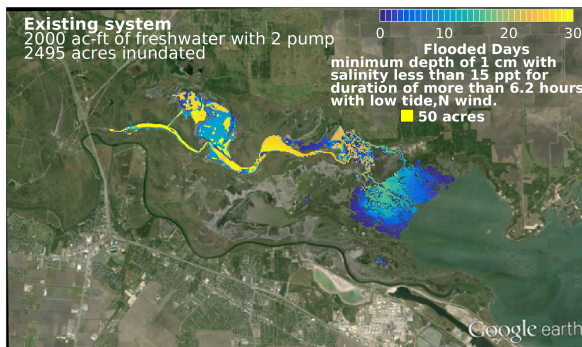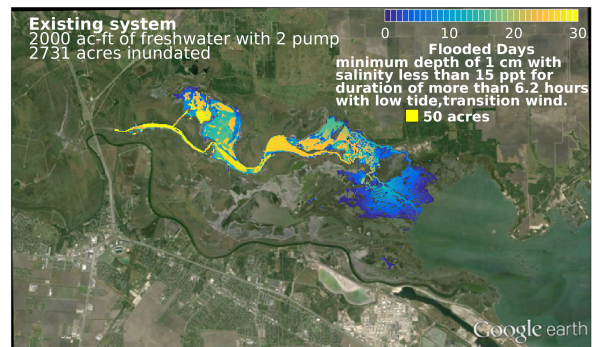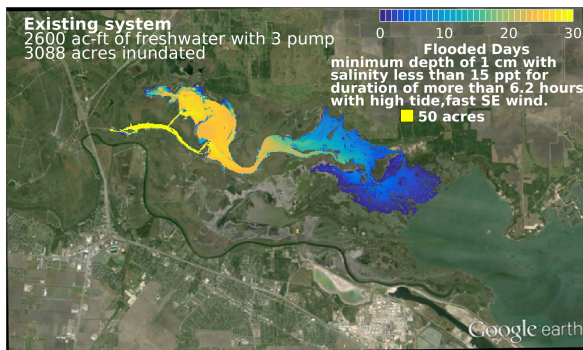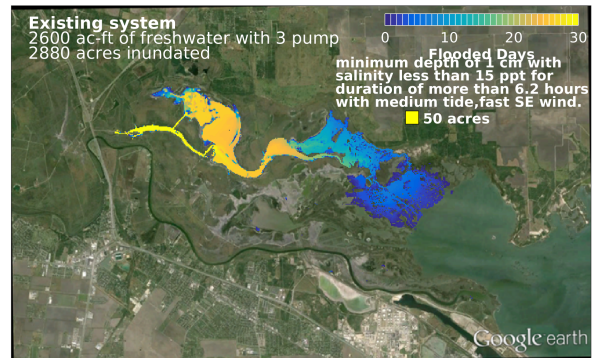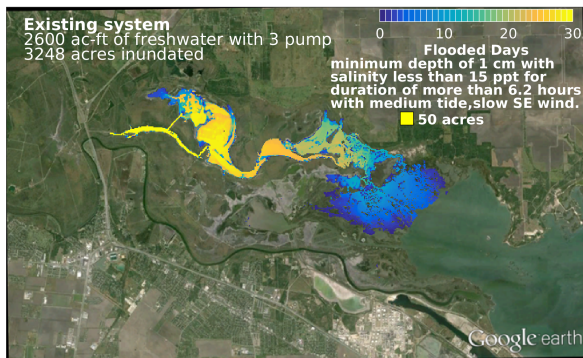

(f) Scenario 6: low tide, slow wind in transition.

Figure 31: Comparison of 3-pump scenarios. Colors indicate days flooded to depth greater than 1 cm with salinities less than 15 ppt for more than 6.2 hours.
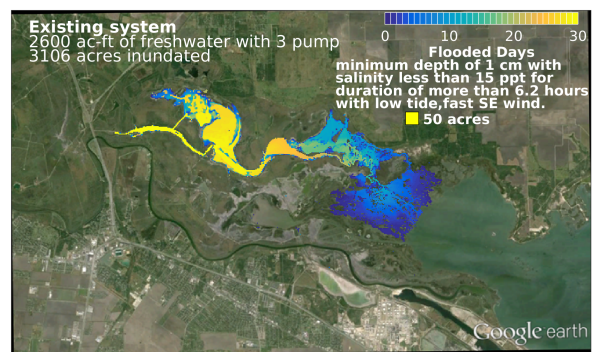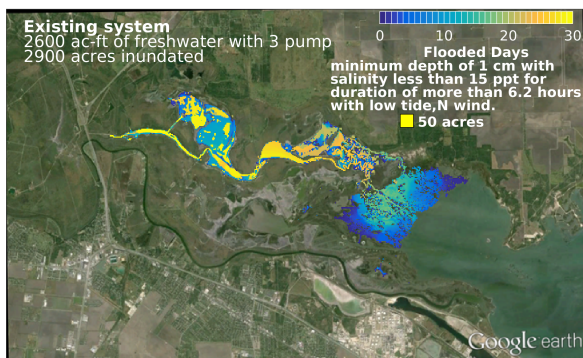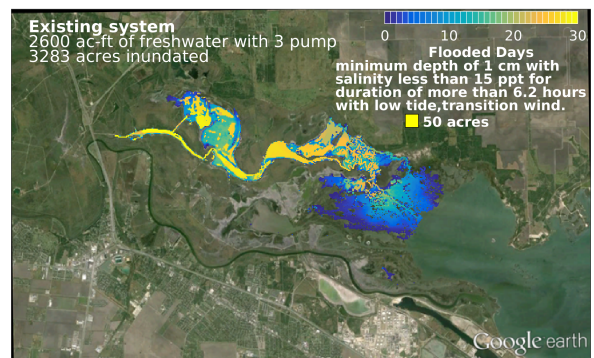
6 Extending the NDHM to Nueces Bay

As a part of this study, we embarked on an effort to extend the NDHM to cover all of Nueces Bay, thereby creating the Nueces Bay and Delta Hydrodynamic Model (NBDHM). The first step of this process was creating a topographic/bathymetric map that combines available lidar data and NOAA bathymetric survies. The resulting bathymetry is shown as Fig. 32. In this process, we discovered that the NOAA bathymetric data set has values in the south central part of Nueces Bay that are clearly wrong as they imply depths greater than 10 m. We filled this area through a manual adjustment and filtering process to obtain a smooth bathymetry that is consistent with the surroundings.
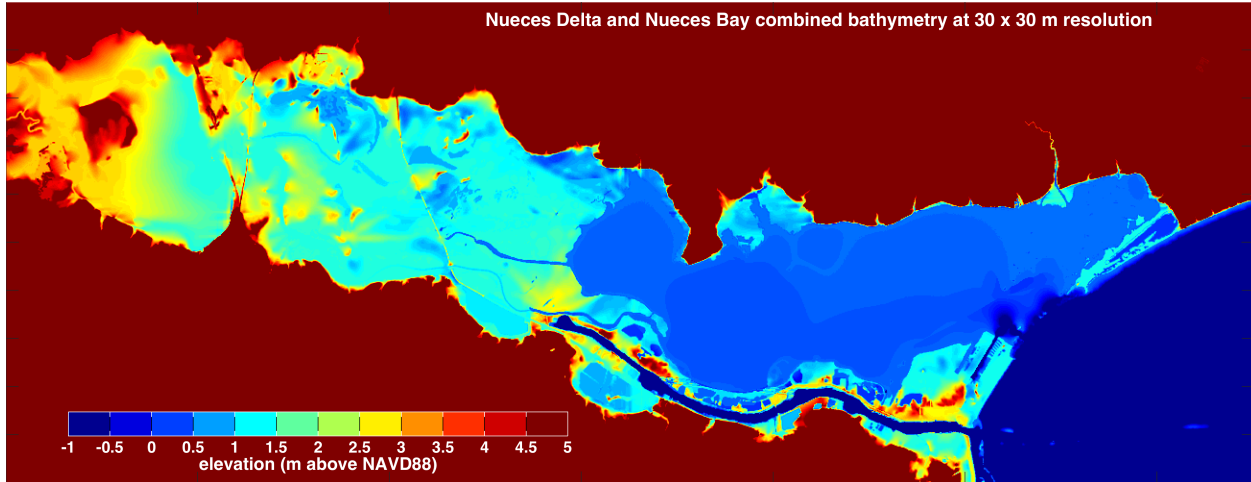

Figure 32: Nueces Bay and Delta combined bathymetry at 30×30 m grid resolution. Note that elevations lower than -1 m and greater than +5 m are truncated in the colormap for clarity.

The second step in model building is testing the Frehd code on the bathymetry with simple tide and wind conditions. Unfortunately, we were not successful in completing this step. Although we have created the basic model, it is essentially unusable due to computational costs. The delta-only model (NDHM) at 30×30 m grid resolution has overall dimensions of 333×485 cells in a 2D space, which corresponds to 161,505 grid cells. Because a large portion of the delta is actually dry, the model only requires solution of water flow in about 25,000 grid cells. In contrast, the combined bay and delta model (NBDHM) has overall dimensions of 501×1301 cells in 2D space, which corresponds to 651,801 grid cells. Because the bay is has more wet flow area than the delta, the combined model requires flow solution over about 250,000 grid cells, which is $10\times$ the requirements of the delta-only model. We have been able to run the delta-only model on 2.9 GHz desktop workstations using about 4GB of RAM and achieved between 5 to 15 times faster than real time on a desktop workstation (depending on the flow conditions). However, the combined delta and bay model dramatically increases the memory requirements and the larger model run times are significantly slower than real time.

The usual solution for high computational costs in a hydrodynamic model is to coarsen the grid scale; however, our experience with the Nueces Delta has convinced us that 30×30 m resolution is the smallest that can be used and retain reasonable representations of the connectivity. To make a substantial reduction in the number of grid cells in the combined delta-bay model would require us to coaresen to 90×90 m grid resolution, which would not adequately represent the delta. To make the problem even more difficult, a principle reason for extending the delta model to Nueces Bay is to capture salinity stratification that might

develop during low wind conditions. Extending the model into 3D with four or five vertical layers puts the cells in the flow solution upwards of 10^6, which we have no hope of being able to achieve using desktop workstations.

There are several possible paths forward. One approach would be to port the underlying Frehd code to a supercomputer so that the bay and delta system can be solved together. A second approach would be to develop a coupled model interface for two separate models – a bay-only model and a delta-only model – so that the models can be run at different grid resolutions (e.g. 90×90 m in the bay and 30×30 m in the delta). A third approach would be to adapt the Frehd code to include provisions for two (or more) grid cell sizes so that the single-model approach could be maintained. The advantage of the supercomputer approach is that it would allow us to retain the simplicity of the uniform Cartesian grid in the present model, but it would inherently tie future modeling to supercomputers. The separate-but-coupled model approach would require the least modification to the Frehd code and so is perhaps the easiest approach to implement; however, coupled model interfaces for fluid flows can be cumbersome an inefficient. Modifying Frehd to include multiple grid sizes requires a change in the storage structure within the code. Although this task is straightforward, it requires a large number of small changes throughout the code and would require extensive debugging. At this point, we do not have a firm recommendation of the best way to proceed. We believe the answer depends on how the TWDB and CBBEP see this model being used in the next 5-10 years.

7 Summary and recommendations for future work

7.1 Calibration and validation

This study has shown that calibration of the NDHM (§3) cannot be accomplished through global changes in the roughness. Indeed, the validation results (§3) show that calibration is irrelevant as the key model errors are driven by (i) additional sources of high salinity, namely evaporation and/or porewater salinity release, and (ii) higher flux rates through narrow channels that are widened to the 30×30 m grid to maintain connectivity, particularly the channel at the connection between the middle Rincon Bayou and North Lake beneath the railroad bridge (Fig. 4). Based on these observations, the next steps recommended for improving the model are (1) deriving a relationship between channel widening and roughness that could be used for slowing the flows in channels that are physically narrower than the model grid resolution, and (2) developing sub-models for evaporation and porewater salinity release that can be used to improve the model validation results. As a minor point, the operation of the gate at the channel between the upper end of the Rincon Bayou and the main stem of the Nueces River needs to be included in the model.

7.2 Freshwater pumping

The key conclusion that can be drawn from the freshwater pumping study (§5) is that a single pump appears to make more effective use of the freshwater than operation of two or three pumps. However, it is also clear that a single pump may not be able to provide freshwater flushing to all the desired areas; that is, the *inundation effectiveness* (acres flooded per acre-foot pumped) is not necessarily the only metric that should be used – there is likely some minimum inundation area that should also be targeted. Under some environmental conditions, a single pump might not be able to provide adequate inundation across broad areas (e.g., lower salt marshes or floodplains to the north of North Lake), so a pumping scheme with a lower inundation effectiveness but higher total coverage area might be preferred.

The freshwater pumping study did *not* provide clear evidence of the relationships between tide, wind speed and wind direction that are optimal for increasing inundation. It seems likely that the interplay be-

47

tween the timing of the wind, tide, and freshwater inflows are critical to understanding these dynamics. To better understand these effects requires more detailed analyses of the wind and tide data during several similar months (perhaps using baselines from Tables 1 and 2), which should be coupled with development of synthetic wind and tide conditions to test hypotheses about the physics that are expected to control the inundation. We suspect that higher tides will tend to increase inundation only when the pumped freshwater is able to reach the saltwater marshes *before* the tide elevation rises. Thus, it might be that two or three pumps operations might be more desirable for obtaining the maximum area so that the freshwater gets to the lower marshes more quickly. Alternatively, it the key might be pump during a *rising* secular tide rather than simply with a *high* secular tide.

7.3 Metrics for inundation

If the TWDB pursues further work with the NDHM in evaluating the freshwater pumping, it would be useful if the TWDB and the CBBEP could define a target inundation acreage (e.g., no less than 2400 ac-ft). Having an area metric for comparison would allow us to discard simulations that are theoretically effective (i.e., with a large inundation effectiveness number), but do not actually flood the areas of interest.

Key problems for such a metric analysis are (1) a substantial part of the acreage is always inundated, and (2) some inundation results are effectively a transfer from one section of the marsh to another. Thus, it is difficult to discriminate between the ecological value of different pumping cases simply by considering acreage alone (as done herein). It might be useful to perform an analysis to determine the commonly submerged acreage (i.e. lakes and channels), which can be subtracted from the total inundation acreage to get an effective inundation increase. Furthermore, it might be useful to define several zones within the delta and compute acreage changes on a zonal basis. With further exploration and refinement of these ideas we might be better able to understand which scenarios are causing flooding to different areas as well as the net effects.

Acknowledgments

References

BBEST. Environmental flows recommendation report. Technical report, Nueces River and Corpus Christi and Baffin Bays Basin and Bay Expert Science Team, 2011.

B.R. Hodges. A new approach to the local time stepping problem for scalar transport. *Ocean Modelling*, 77:1–19, 2014.

B.R. Hodges. Representing hydrodynamically important blocking features in coastal or riverine lidar topography. *Natural Hazards and Earth System Sciences*, 2015.

B.R. Hodges and F.J. Rueda. Semi-implicit two-level predictor-corrector methods for non-linearly coupled, hydrostatic, barotropic/baroclinic flows. *International Journal of Computational Fluid Dynamics*, 22(9): 593–607, 2008.

B.R. Hodges, J. Imberger, A Saggio, and K. Winters. Modeling basin-scale internal waves in a stratified lake. *Limnology and Oceanography*, 45(7):1603–1620, 2000.

B.R. Hodges, K.H. Dunton, P.A. Montagna, and G.H. Ward. Nueces delta restoration study. Technical report, institution, 2012.

B. Laval, J. Imberger, B.R. Hodges, and R. Stocker. Modeling circulation in lakes: spatial and temporal variations. *Limnology and Oceanography*, 48(3):983–994, 2003.

L Lloyd, J.W. Tunnell, and A Everett. Nueces delta salinity effects from pumping freshwater into the rincon bayou: 2009 to 2013. Technical report, institution, 2013.

G.B. Pasternack, A.T. Gilbert, J.M. Wheaton, and Buckland E.M. Error propagation for velocity and shear stress prediction using 2d models for environmental management. *Journal fo Hydrology*, 328:227–241, 2006.

F.J. Rueda, E. Sanmiguel-Rojas, and B.R. Hodges. Baroclinic stability for a family of two-level, semi-implicit numerical methods for the 3d shallow water equations. *International Journal of Numerical Methods in Fluids*, 54(3):237–268, 2007.

A.J. Ryan and B.R. Hodges. Modeling hydrodynamic fluxes in the nueces river delta. Technical report, University of Texas at Austin, 2011a.

A.J. Ryan and B.R. Hodges. Users guide to the nueces delta hydrodynamic model v1.0. Technical report, University of Texas at Austin, 2011b.

C Schoenbaechler, S Negusse, and C.G. Guthrie. Nueces delta data collection for calibration and validation of the nueces delta hydrodynamic model. Technical report, Bay and Estuaries Program, Surface Water Resources Division, Texas Water Development Board, 2014.

B.M. Wadzuk and B.R. Hodges. Hydrostatic versus nonhydrostatic euler-equation modeling of nonlinear internal waves. *Journal of Engineering Mechanics*, 135(10):1069–1080, 2009.

G.H. Ward. Processes and trends of circulation with the corpus christi bay national estuary program study area. Technical report, Corpus Christ Bay National Estuary Program, 1997.

L. White and B.R. Hodges. Filtering the signature of submerged large woody debris from bathymetry data. *Journal of Hydrology*, 309(1-4):53–65, 2005.